

Growth and textural ageing in long bones of the American alligator *Alligator mississippiensis* (Crocodylia: Alligatoridae)

ALLISON R. TUMARKIN-DERATZIAN¹*, DAVID R. VANN² and PETER DODSON^{2,3}

¹Department of Geology and Geography, Vassar College, Poughkeepsie, New York, USA

²Department of Earth and Environmental Science, University of Pennsylvania, Philadelphia, Pennsylvania, USA

³Department of Animal Biology, School of Veterinary Medicine, University of Pennsylvania, Philadelphia, Pennsylvania, USA

Received December 2004; accepted for publication June 2006

Growth series of femora, tibiae, and humeri of the American alligator *Alligator mississippiensis* were examined to assess the relationship between bone surface textures and relative skeletal maturity. Element texture types were compared with both size-based and size-independent maturity estimates. Selected elements were thin sectioned to observe the histological structures underlying various surface textures. Results suggest little to no relationship between bone textures and skeletal maturity in *Alligator*. Controlling for additional factors suspected to affect textural variation – sexual dimorphism, seasonally interrupted growth, wild vs. captive habitat, and geographical range – provides little resolution. Indeterminate growth is almost certainly a factor; however, this alone cannot explain all observed variability. Histological analyses reveal that highly porous surface textures are often associated with zones composed of fibrolamellar bone; smoother textures are generally underlain by lamellar zones or annuli. Textures of intermediate porosity may be associated with more than one histological pattern. Until the factors affecting bone texture changes in modern crocodylians are better understood, it is recommended that the textural ageing method be applied with caution to studies of fossil archosaurs with crocodylian-like or unknown growth regimes. © 2007 The Linnean Society of London, *Zoological Journal of the Linnean Society*, 2007, **150**, 1–39.

ADDITIONAL KEYWORDS: crocodylian – histology – maturity – ontogeny – skeleton.

INTRODUCTION

A potential method for assessing relative ontogenetic age of vertebrate skeletal material relies on distinguishing between immature (juvenile and subadult) and mature (adult) textures on bone surfaces. It should be stressed that in this context the terms ‘immature’ and ‘mature’ are meant only to designate stages in the growth and development of the skeleton, without implying any connection to sexual development or reproductive status. Generalized changes in bone surface textures with increasing ontogenetic age have

been noted for a variety of fossil reptiles, including ichthyosaurs (Johnson, 1977), pelycosaur (Brinkman, 1988), pterosaurs (Bennett, 1993) and dinosaurs (Callison & Quimby, 1984; Jacobs *et al.*, 1994; Sampson, Ryan & Tanke, 1997; Carr, 1999; Brill & Carpenter, 2001; Ryan *et al.*, 2001; Ryan & Russell, 2005).

Surface textural variations in fossil taxa have been viewed as macroscopic reflections of degree of ossification and vascularization of immature vs. mature skeletal material. Immature textures are presumed to be linked to rapid bone growth in early ontogeny; adult bone texture is attributed to a later slowing or cessation of growth (Johnson, 1977; Bennett, 1993; Sampson *et al.*, 1997; Ryan *et al.*, 2001). Bennett’s (1993) pterosaur study, however, provides the only detailed account relating macroscopic textures in fossil vertebrates to underlying histological features. The porous

*Corresponding author. Current address: Temple University, Department of Geology, Beury Hall (016-00), 1901 North 13th Street, Philadelphia, PA 19122-0681, USA.
E-mail: altd@temple.edu

immature texture results from penetration of the bone surface by vascular canals in underlying fibrolamellar bone; the non-porous mature texture is underlain by less vascular lamellar bone deposited as individuals attain skeletal maturity and growth rates slow (Bennett, 1993). Histological ontogenetic studies of several archosaur taxa (Chinsamy, 1990, 1993; de Ricqlès, Padian & Horner, 1993; Varricchio, 1993; Horner & Currie, 1994; Chinsamy, 1995; Curry, 1999; de Ricqlès *et al.*, 2000; Horner, de Ricqlès & Padian, 2000; Sander, 2000; Chinsamy & Elzanowski, 2001; de Ricqlès, Padian & Horner, 2001; Horner, Padian & de Ricqlès, 2001; de Ricqlès *et al.*, 2003; Padian, Horner & de Ricqlès, 2004) document decreasing vascularization in the outer cortex with increasing age. These changes suggest decreasing growth rates and are probably associated with textural changes on a macroscopic level. With one exception (Horner & Currie, 1994), the authors of the histology studies do not address this possible link with surface textures.

An understanding of the relationship between texture and skeletal maturity in modern taxa is necessary before the textural ageing method can be reliably applied to fossils. Crucial issues are whether surface textures do in fact change in a predictable manner during ontogeny, whether a single set of textural criteria may be applicable across taxa, the effect of general growth regime on textural changes, and the underlying histological features associated with different textural patterns. Treatments of ontogenetic textural change in modern archosaurian taxa have largely considered birds; studies have examined both zooarchaeological samples (Benecke, 1993; Cohen & Serjeantson, 1996; Gotfredsen, 1997; Serjeantson, 1998; Mannermaa, 2002; Serjeantson, 2002) and recent skeletal material (Callison & Quimby, 1984; Sanz *et al.*, 1997; Serjeantson, 1998; Mannermaa, 2002; Serjeantson, 2002; Tumarkin-Deratzian, Vann & Dodson, 2006). Tumarkin-Deratzian *et al.* (2006) examine textural change patterns and associated histological features in the Canada goose *Branta canadensis*. Their results are similar to those reported by Bennett (1993) for pterodactyloid pterosaurs; a gradual decrease in porous textures throughout ontogeny corresponds to a shift from fibrolamellar to lamellar bone deposition as growth slows. Ontogenetic bone texture change in modern or fossil crocodylians has not been addressed in detail, although Johnson (1977) postulates, but does not test for, the existence of a pitted subperiosteal texture on the actively growing bone of young individuals, and a smooth surface in older animals in which appositional growth has slowed.

The present study aims to continue the investigation of texture changes in modern archosaurs begun with the *Branta* project, by examining in detail the relationship between surface texture, bone histology

and skeletal maturity in the American alligator *Alligator mississippiensis* Daudin. *Alligator mississippiensis* was selected as the representative crocodylian species for several reasons, including the fact that it is the most common and widespread crocodylian species in the United States (Groomsbridge, 1987; Joanen & McNease, 1987b). More importantly, however, the life history and general growth patterns of *A. mississippiensis*, both in the wild and in captivity, have been the focus of numerous previous studies (e.g. McIlhenny, 1935; Bellairs, 1970; Neill, 1971; Dodson, 1975; Chabreck & Joanen, 1979; Wink & Elsey, 1986; Joanen & McNease, 1987a, b; Wink, Elsey & Hill, 1987; Jacobsen & Kushlan, 1989; Magnusson *et al.*, 1989; Elsey *et al.*, 1990; Rootes *et al.*, 1991; Woodward, White & Linda, 1995; Brochu, 1996; Dalrymple, 1996; Wilkinson & Rhodes, 1997; Elsey, Lance & McNease, 2000a; Elsey, McNease & Joanen, 2000b; Lance, Morici & Elsey, 2000; Huchzermeyer, 2002; Richardson, Webb & Manolis, 2002; Farlow *et al.*, 2003, 2005; Lance, 2003); thus there exists a large knowledge base addressing the biology of this taxon.

Individuals hatch with a body length of 200–220 mm (femur length approximately 20 mm). Both sexes grow at approximately the same rate (roughly 200 mm per year) until age 3 years, after which growth rates in females progressively decrease relative to those in males. Individuals are generally sexually mature at body lengths of 1.8–1.9 m; this size is reached at an earlier age in males than in females. Chronological age of females at sexual maturity also varies due to geographical variation in growth rates throughout the species' range. Females appear to reach a maximum length of 2.7–3.1 m. Estimated maximum length for males is 4.3–4.57 m (Woodward *et al.*, 1995), although this may represent current mortality trends rather than an actual upper size limit given that animals of up to 5.5 m have been reported in the past (Neill, 1971). Growth in *Alligator mississippiensis* is indeterminate; thus, attainment of 'maximum length' does not necessarily mean that growth has stopped altogether, but that it has slowed to a point as to be nearly imperceptible grossly (McIlhenny, 1935; Neill, 1971; Andrews, 1982).

Growth in *Alligator mississippiensis* is further mediated by seasonal factors such as temperature and food availability such that a period of slowed or arrested growth occurs during the winter season (Peabody, 1961; Enlow, 1969; Neill, 1971; Chabreck & Joanen, 1979; Andrews, 1982; Castanet *et al.*, 1993). These seasonal variations in growth rate are visible histologically as lamellar-zonal bone comprising zones and annuli and/or lines of arrested growth (LAGs) (Enlow & Brown, 1957; Peabody, 1961; Enlow, 1969; de Ricqlès, 1974, 1976; de Buffrenil, 1980a, b; Reid, 1984, 1990; Castanet *et al.*, 1993; Castanet, 1994; Chinsamy

& Dodson, 1995; Chinsamy, Chiappe & Dodson, 1995). Zones are vascularized regions deposited during the active growing season. They are most often documented as regions of lamellar or pseudolamellar bone, although fibrolamellar bone may also form when growth is relatively rapid, as in young individuals and captive animals raised under optimum conditions (Enlow, 1969; de Buffrenil, 1980b; Reid, 1990; Castanet *et al.*, 1993; Castanet, 1994; Chinsamy & Dodson, 1995; Reid, 1997a, b, c; Horner *et al.*, 2001; de Ricqlès *et al.*, 2003; Padian *et al.*, 2004). Annuli comprise thinner, sparsely vascularized or avascular sheets of lamellar bone deposited during periods when growth has slowed. LAGs, as their name implies, are rest lines formed during a hiatus in growth. These histological features have also been documented in captive crocodylians living under more-or-less constant conditions, although they are not as pronounced as in wild individuals (de Buffrenil, 1980b).

INSTITUTIONAL ABBREVIATIONS

FWC, Florida Fish and Wildlife Conservation Commission; MOR, Museum of the Rockies, Bozeman, Montana; ROM, Royal Ontario Museum, Toronto; UF, Florida Museum of Natural History, University of Florida, Gainesville.

MATERIAL AND METHODS

Alligator mississippiensis long bones in osteological collections of the ROM, MOR and UF were surveyed.

The UF collection was further supplemented with bones obtained in co-operation with the FWC during study of a die-off of animals on Lake Griffin, Lake County, Florida (Ross *et al.*, 2002; Schoeb *et al.*, 2002), during spring and summer 2000. The FWC sample includes bones salvaged from carcasses on Lake Griffin, as well as fresh limbs taken from animals necropsied by the FWC. Individuals are identified by FWC tag numbers where these were recovered. Untagged individuals are designated with the prefix Lake Griffin Study (LGS). The total study sample comprises 109 individuals drawn from multiple populations in Florida, Louisiana and South Carolina (Table 1). Femur lengths of sampled individuals range in size from 19.41 to 270.14 mm. Effort was made initially to include only individuals for which sex, season of death, habitat and locality data were known, although some individuals with incomplete data were eventually included to increase the sample size. Femur, tibia and humerus were examined for each individual as available; the MOR sample consisted only of femora. Preference was given to right side elements; left elements were used in cases where the right was missing, damaged *post mortem* or pathologic.

ANATOMICAL TERMINOLOGY

Directional terms used here follow the conventions of the *Nomina Anatomica Veterinaria* (Sack & Habel, 1994) and Meers (2003); thus, the terms 'cranial' and 'caudal' are substituted for 'anterior' and 'posterior' as sporadically found in the literature. Directional terms

Table 1. Source localities and habitats of study sample individuals

State	County/Parish	Number of individuals				
		Total	Wild	Captive	Farm	Unknown
Florida		49				
	Alachua	1	1			
	Broward	2	2			
	Highlands	10			10	
	Lake	11	11			
	Palm Beach	10	10			
	Polk	1	1			
	Putnam	1	1			
	Saint Johns	4	4			
	Volusia	8	8			
	Unknown	1				1
Louisiana		56				
	Cameron	56	21	35		
South Carolina		3				
	Aiken	3				3
Unknown		1	1			

pertaining to surfaces of the femur and humerus are inconsistent in the crocodylian literature, as a result of the variable orientations of these bones depending on the animal's limb posture. In a sprawling posture, femur and humerus have nearly horizontal orientations, with dorsal, ventral, cranial and caudal surfaces. When the animal assumes a more upright limb posture, femur and humerus adopt more vertical orientations, with cranial, caudal, medial and lateral surfaces. Cranial and caudal surfaces on the femur are analogous in both postures; the humerus rotates when shifting posture such that no directions correspond. To allow for the broadest comparability with other studies, directional terms for both postures are used here with the format 'upright orientation (sprawling orientation)' in cases where directions differ between postures. The femur therefore has the following surfaces: cranial, caudal, medial (ventral) and lateral (dorsal). Surfaces of the humerus are cranial (ventral), caudal (dorsal), medial (caudal) and lateral (cranial).

SEASON AND HABITAT CODES

Due to the likely association between surface textures and bone growth patterns (Johnson, 1977; Bennett, 1993; Sampson *et al.*, 1997; Ryan *et al.*, 2001; Tumarkin-Deratzian *et al.*, 2006), death of individuals during active vs. inactive growth periods is potentially important. For *Alligator mississippiensis*, the winter season of slowed or arrested growth varies somewhat throughout the species' range, but generally lasts from October or November to March (Neill, 1971; Chabreck & Joanen, 1979; Wilkinson & Rhodes, 1997; J.P. Ross, pers. comm., 2000). For the purposes of this study, three seasons of death were distinguished: an inactive season (November–March), a transitional season (April and October) and an active season (May–September). The transitional period was erected as an attempt to account for geographical and yearly variation in durations of active and inactive growth periods.

Habitat was classified as wild, captive or farm. Captive animals were raised under ambient light and temperature conditions in large enclosures allowing for normal mobility. Farm-raised animals were confined in tanks under controlled temperature and light conditions. Two wild individuals (MOR HIP2001-08R-40 and MOR HIP2001-08R-41) placed in captivity in 1993 until death in 1999 were coded as captive. All captive and farm-raised animals died within the designated active growth season. No adjustment was therefore made to reflect the fact that these individuals may have experienced more constant growing conditions, and therefore no true periods of inactive growth, relative to their wild counterparts.

ESTIMATING SKELETAL MATURITY

Relative skeletal maturity of individuals in the study sample was estimated by three independent methods (one size-based, two size-independent). The size-based estimate used femur length [measured from the most proximal point on the femoral head to the most distal point on the lateral (dorsal) condyle] as a proxy for overall size of the individual, following studies by Dodson (1975) and Farlow *et al.* (2003, 2005). Relative body size was then employed as an estimate of relative age and skeletal maturity. Size-based age estimates, however, are often problematic in *Alligator mississippiensis*, due to variation in size and/or growth rates between sexes and among habitats and geographical regions (McIlhenny, 1935; Peabody, 1961; Bellairs, 1970; Neill, 1971; Chabreck & Joanen, 1979; Andrews, 1982; Jacobsen & Kushlan, 1989; Magnusson *et al.*, 1989; Rootes *et al.*, 1991; Castanet *et al.*, 1993; Woodward *et al.*, 1995; Dalrymple, 1996; Wilkinson & Rhodes, 1997). Sex and geographical region were known for the majority of the study sample; variation due to other factors could not be controlled for in the collections examined. Due to the difficulties inherent in a size-based analysis, additional, size-independent, age estimates were used. Character matrices were constructed for each element based on presence/absence data for muscle scars and other bony landmarks visible in the largest and thus presumably oldest animals. Characters and character states employed here are adapted from those used by Brochu (1992, 1996); these are illustrated in Figure 1 and summarized in Appendix 1. A feature was considered present if it was visible under a 10× hand lens. Bone landmark data were analysed by two separate methods.

The first method was a modified version of that designed by Brochu (1992, 1996) to determine ontogenetic transformation series for *Alligator mississippiensis* appendicular bones. Multiple individuals with identical suites of character states were omitted from the matrix to reduce volume in the data set. Ontogenetic matrices were subjected to parsimony analysis using the branch and bound algorithm of PAUP, version 4.0b10 (Swofford, 1999). The outgroup was coded as a hypothetical embryonic form lacking all bony landmarks considered. More than one most parsimonious tree was obtained in all cases; a strict consensus tree was generated to identify those nodes present in all trees. Only character appearances associated with the consistent nodes were treated as representing discrete ontogenetic stages. Characters showing reversals or multiple independent appearances were discarded as unreliable indicators. The remaining characters were those that consistently appeared in a predictable order during ontogeny. Based on this

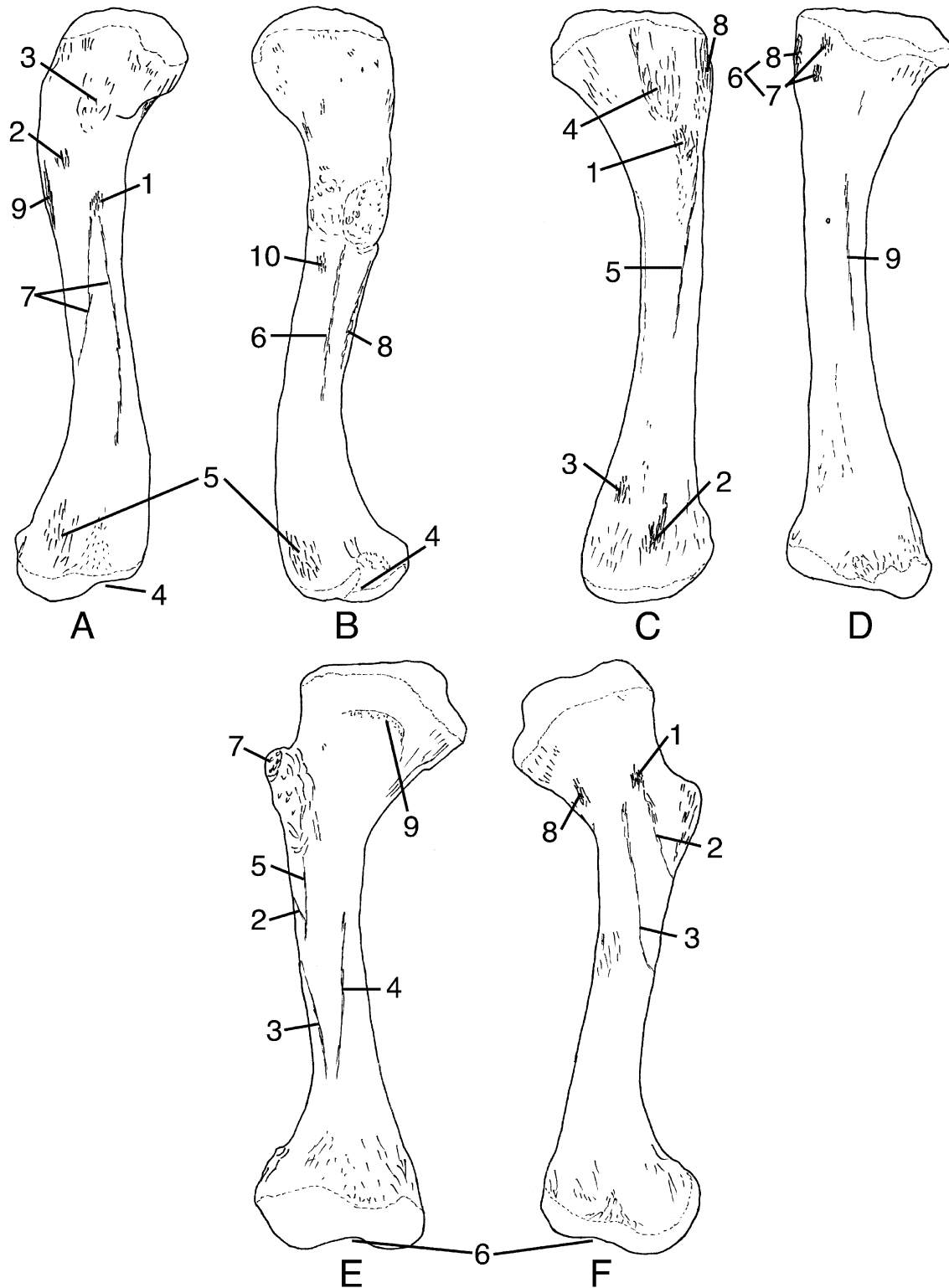


Figure 1. Diagrammatic representation of *Alligator* long bones illustrating bone landmarks used in determining size-independent maturity estimates. Elements are all drawn to the same scale and are not in proportion to one another as they would be in a single individual. Numbers correspond to character definitions in Appendix 1. A, femur, craniolateral (craniodorsal) view. B, femur, caudomedial (caudoventral) view. C, tibia, cranial view. D, tibia, caudal view. E, humerus, cranial (ventral) view. F, humerus, caudolateral (dorsocranial) view.

series, the ontogenetic status (percentage maturity) of any given element from a particular skeleton could be expressed as a percentage of the total number of stages through which that element must pass before attaining full maturity. A bone at stage 2 out of four total stages, for example, received a percentage maturity value of 50%.

The second analytical method used hierarchical clustering analysis to test for natural groups of specimens with similar characters. As the presence/absence data are binary states, a normalized percent disagreement metric was used as the distance metric. The linkage method used was complete (farthest neighbour), because the individual characters are assumed to accumulate with age. Ontogenetic stages recognized by the cluster analysis were then converted to percentage maturity values following the same procedure used for the parsimony-based stages.

It should be stressed that in neither case does the percentage maturity value imply temporal equivalence in length of ontogenetic stages. Designation of a bone as 50% mature, for example, means only that it has passed through half of the ontogenetic stages recognizable for that bone. This does not necessarily equate to 'half-grown' in a temporal sense, as different ontogenetic stages may have different durations with respect to the lifespan of the individual.

Experimental studies have demonstrated that annuli and LAGs represent annual features in crocodylian bone (de Buffrenil, 1980a; Hutton, 1986; Tucker, 1997). A count of these features in thin section may therefore provide a minimum absolute age estimate for the individual (Peabody, 1961; de Buffrenil, 1980a, b; Castanet, 1987, 1994; Castanet *et al.*, 1993; Tucker, 1997). Skeletochronological ages obtained in this manner are minimum estimates because resorption of the inner layers of cortical bone destroys evidence of earlier growth cycles. Such resorption occurs in all individuals during growth, but is particularly notable in females of reproductive age (Enlow, 1969; Wink & Elsey, 1986; Castanet, 1987; Wink *et al.*, 1987; Brochu, 1996). Due to the fact that most bones in the study sample were not available for thin sectioning, skeletochronology was only employed in selected cases to estimate age within the portion of the FWC sample selected for histological analysis.

SURFACE TEXTURE CODING

All specimens were examined grossly with the unaided eye and a 10× hand lens. Surface patterns for each bone were documented qualitatively through a combination of detailed description, sketches and photography. In determining major textural types, femora, tibiae and humeri were analysed as separate subsamples without any reference to size and age data

or skeletal maturity estimates. Bones within each element subsample were grouped based on similar surface patterns; textural types for that element were then defined based on characteristic surface patterns of each group. Types were ordered based on decreasing surface porosity. Within this spectrum, a numerical texture code was then assigned to each individual bone. Relationships between skeletal maturity and texture type were evaluated only after these values were assigned.

RELATIONSHIP BETWEEN TEXTURE TYPE AND ONTOGENY

In order to address the relationships between femur length as a body size proxy and percentage maturity, and between texture type and body size, the data were analysed using a one-way fixed-effects ANOVA. Post-hoc differences among groups were tested via Tukey's test. The large differences in replicate number between the various classes cause a violation of the assumption of equal variances; therefore, the data were also analysed via Kruskal–Wallis ANOVA on Ranks, with Dunn's procedure for post-hoc analysis. The relationship between texture type and cluster-based ontogenetic stage was also analysed using a two-way ranked-order contingency table. The values for Pearson's χ^2 (Chi-squared), Spearman's ρ (Rho) and Goodman-Kruskal's γ (Gamma) statistics were determined. Chi-squared tests whether the two categories are independent. Rho tests the same question using rank indices rather than actual data; it is thus independent of sample size influences. Gamma tests whether the prediction of the value of one category is improved by knowledge of the other category. More sophisticated model-testing approaches were not available, as the sample sizes of the smaller and less mature individuals were too small for reliable testing. Consequently, further conclusions regarding the relationship between bone surface texture and ontogeny were made based on visual inspection of texture type vs. size and percentage maturity plots.

HISTOLOGICAL THIN SECTIONS

Representatives of different textural types were selected from the FWC sample for analysis of histological features underlying various surface patterns. After removal of most skin and muscle, all bones were heated in a solution of mild detergent, scrubbed with a soft brush to remove remaining non-osseous tissue and air-dried.

Transverse thin sections from five regions of each bone (Fig. 2) were prepared undecalcified following a modification of methods outlined for fossil bone by Chinsamy & Raath (1992). Segments of bone surrounding the desired section locations were cut on a

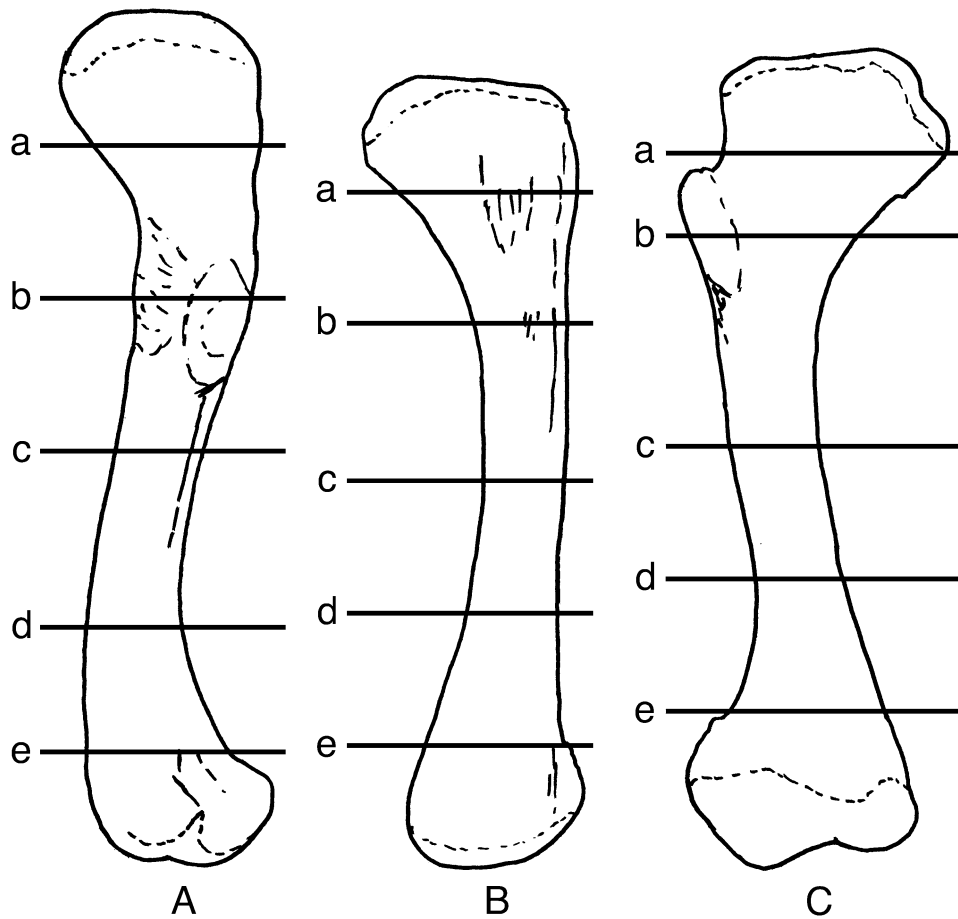


Figure 2. Diagrammatic representation of *Alligator* long bones showing locations of thin sections used in histological analyses in relation to major bone contours. Elements are all drawn to the same scale and are not in proportion to one another as they would be in a single individual. A, femur, caudomedial (caudoventral) view. B, tibia, cranial view. C, humerus, cranial (ventral) view.

circular diamond saw, then embedded in resin under vacuum prior to further cutting. Embedded segments were first divided into lateral and medial halves (based on upright posture orientations), to reduce distortion during mounting. From each half-segment was cut a wafer 3 mm in thickness, of which one surface was the desired plane of section for that segment. During this process, freshly exposed surfaces were coated under vacuum with Paleo-Bond penetrant stabilizer after each cut. Treated surfaces were allowed to set for 24 h to seal any opened pores and improve stability of the sample.

The surface of the wafer corresponding to the desired plane of section was ground smooth on a graded sequence of 320–600 grit silicon carbide grinding paper, then mounted on a frosted plastic slide using low-viscosity cyanoacrylate adhesive. Excess wafer was then ground away on a graduated series of 180, 320 and 600 grit silicon carbide papers until

desired section thickness was attained. Sections were ground until the desired cellular structures were visible under the microscope, rather than to a standard measured thickness. Thin sections were examined by light microscopy to determine histological correlates of gross surface patterns.

RESULTS

SIZE-INDEPENDENT MATURITY ESTIMATES

Strict consensus trees derived from parsimony analyses of femora, tibiae and humeri are shown in Figure 3. Including the hypothetical embryonic stage (designated stage 0 for all three elements), the analyses yielded transformation series of four stages for the femur, three for the tibia and two for the humerus. Stages and their defining characters are summarized in Table 2. Character definitions for each stage are

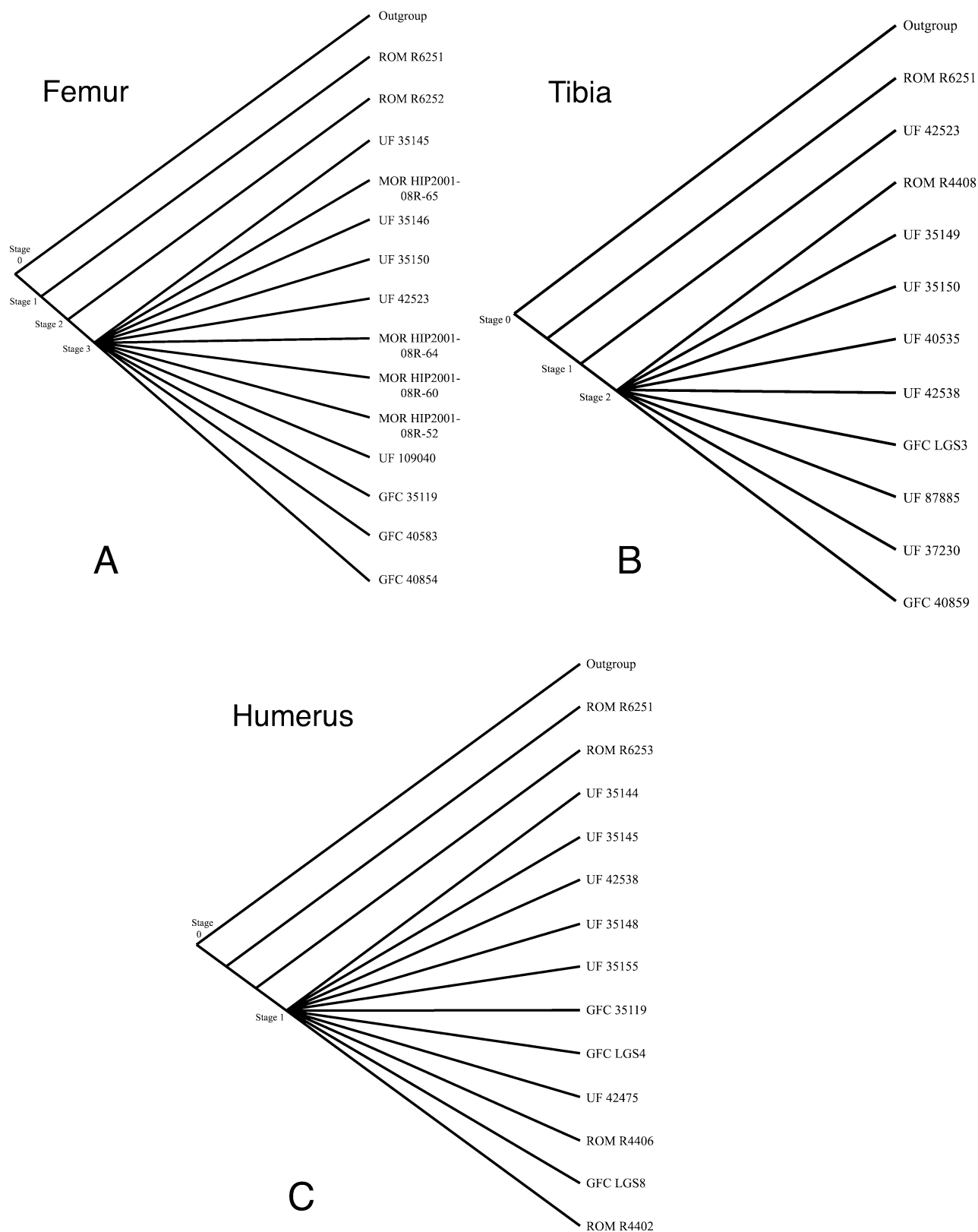


Figure 3. Strict consensus trees resulting from parsimony analyses. Numbered ontogenetic stages are defined in Table 2. A, femur: strict consensus of 34 281 trees, tree length = 18, CI = 0.3846. B, tibia: strict consensus of 357 trees, tree length = 13, CI = 0.5077. C, humerus: strict consensus of 36 trees, tree length = 15, CI = 0.4286.

Table 2. Ontogenetic stages as determined by parsimony analysis. Character acquisition is cumulative: Stage 2 possesses characters listed for Stages 1 and 2, etc. Numbers in parentheses indicate character numbers as listed in Appendix 1

Stage	Definition	Percentage maturity
Femur		
0	Absence of all coded characters	0
1	Appearance of: Medial scar for <i>M. puboischiofemoralis internus</i> , pars dorsalis (1)	33
2	Appearance of: Lateral scar for <i>M. puboischiofemoralis internus</i> , pars dorsalis (2)	67
3	Appearance of: Distal trochlea (4) Rugosity on medial and lateral sides of distal condyle (5) Longitudinal scars for <i>M. iliofemoralis</i> (7)	100
Tibia		
0	Absence of all coded characters	0
1	Appearance of: Scar for medial tibioastragalar ligament (2) Scar for <i>M. interosseus cruris</i> (3) Scar for internal lateral ligament (4) Assemblage of scars for <i>M. tibialis caudalis</i> , <i>M. tibialis cranialis</i> , and femorotibial ligament (6)	50
2	Appearance of: Scar for <i>M. flexor tibialis interior</i> (1)	100
Humerus		
0	Absence of all coded characters	0
1	Appearance of: Scar for <i>M. teres major</i> and branch of <i>M. latissimus dorsi</i> (1) Scar for <i>M. humeroradialis</i> (3)	100

cumulative: stage 1 is defined by presence of the characters listed, stage 2 by presence of all the characters for stage 1 plus the defining characters of stage 2, and so on. The results for the current sample differ from those of Brochu (1996), who recognized seven stages for the femur, five for the tibia and three for the humerus. This may be a consequence of the larger sample size (109 vs. 48 individuals) used in the present study.

Results of the cluster analyses are shown in Figure 4; cluster-based ontogenetic stages are defined in Table 3. Including stage 0 lacking all characters, five ontogenetic stages are recognized for the femur, four for the tibia and four for the humerus. As with the parsimony analysis, character acquisitions among stages are, for the most part, cumulative.

Femoral cluster-based stages 0 and 1 are defined by the same character states as the equivalently numbered parsimony-based stages (Tables 2, 3). Cluster-based stage 2 is equivalent to parsimony-based stage 3. [Individuals in parsimony-based stage 2, defined by appearance of character 2 (lateral scar for *M. puboischiofemoralis internus*, pars dorsalis), are included within cluster-based stage 1.] The cluster analysis rec-

ognizes two additional stages for the femur (cluster-based stages 3 and 4), defined by the acquisition of characters 9 (tertiary longitudinal scar) and 10 (distinct scar for *M. puboischiofemoralis internus*, pars medialis), respectively. Four individuals express anomalous conditions of character 9. UF 35146 and UF 109040 have character 9 although based on the absence of character 8 they are placed in stage 2; FWC 40583 and UF 42523 lack character 9 but are placed in stage 4 based on the presence of character 10.

Tibial cluster-based stages 0 and 1 are defined by the same characters as the parsimony-based stages of the same number (Tables 2, 3). Cluster-based stage 2 is defined by the acquisition of character 5 (ridge for *M. tibialis cranialis* extending from *M. flexor tibialis interior* scar), as opposed to parsimony-based stage 2, which is defined by character 1 (scar for *M. flexor tibialis interior*). This change in definition results in the shift of 15 individuals from stage 2 (parsimony-based) to stage 1 (cluster-based). Thus, although stage 1 is defined by acquisition of the same characters in both analyses, it does not include the same set of individuals. The cluster analysis also recognizes an additional stage 3, not recognized by the parsimony analysis,

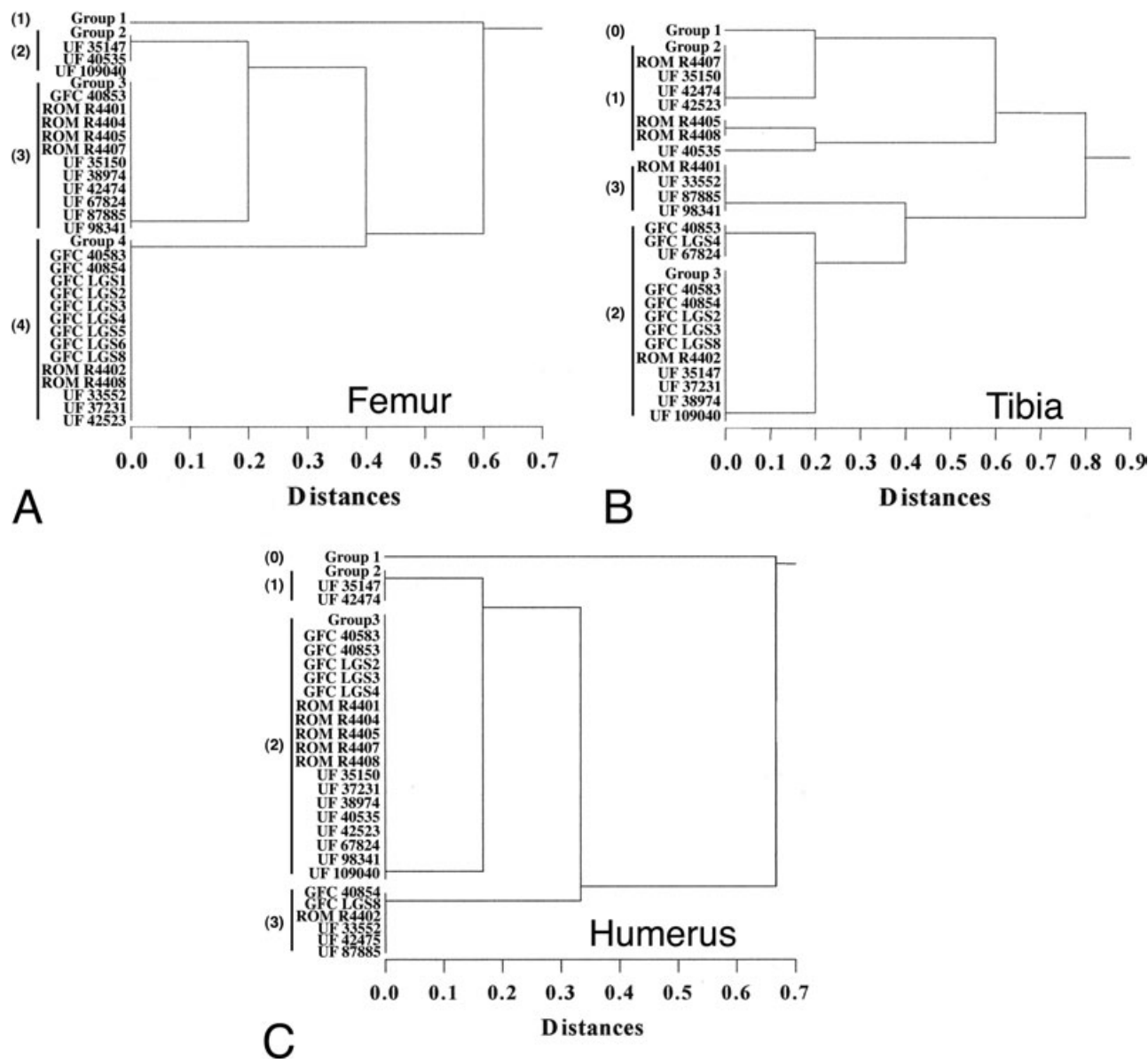


Figure 4. Consensus results of cluster analyses of bone landmark characters. Distance metric is normalized percent disagreement. Complete linkage method (farthest neighbour). Numbers in parentheses represent ontogenetic stages. 'Groups' represent individuals of the same ontogenetic stage grouped together to reduce the size of the trees; included individuals are listed in Appendix 2. A, femur: tree based on distributions of characters 1, 4, 5, 8 and 10. B, tibia: tree based on distributions of characters 5, 6, 7, 8 and 9. C, humerus: tree based on distributions of characters 1, 3, 4, 6, 7 and 8.

defined by acquisition of character 7 (scars for femorotibial ligament and *M. tibialis caudalis* distinct from the assemblage also containing scar for *M. tibialis cranialis*). UF 40523 and UF 42538 both have character 7, but are placed in cluster stage 1 due to an absence of character 5, the defining feature of cluster stage 2. FWC 40859 shows an ambiguous state for character 7; it is therefore assigned to stage 2. ROM R6251 is placed in stage 0 in spite of the presence of one character (character 9, posterior ridge for *M. flexor digi-*

torum longus). Based on the distribution of character 9 in the rest of the sample, its occurrence in ROM R6251 in the absence of any other characters is believed to be anomalous.

Humeral cluster-based stage 0 includes only three individuals (ROM R6251, R6252, R6253), all documented hatchlings. It is best defined by the absence of all characters diagnostic of later stages, since ROM R6252 lacks all characters, ROM R6251 possesses character 2 only, and ROM R6253 exhibits characters

Table 3. Ontogenetic stages as determined by cluster analysis. Character acquisition is cumulative. Numbers in parentheses indicate character numbers as listed in Appendix 1

Stage	Definition	Percentage maturity
Femur		
0	Absence of all coded characters	0
1	Appearance of: Medial scar for <i>M. puboischiofemoralis internus</i> , pars dorsalis (1)	25
2	Appearance of: Distal trochlea (4) Rugosity on medial and lateral sides of distal condyle (5) Longitudinal scars for <i>M. iliofemoralis</i> (7)	50
3	Appearance of: Tertiary longitudinal scar (9)	75
4	Appearance of: Distinct scar for <i>M. puboischiofemoralis internus</i> , pars medialis (10)	100
Tibia		
0	Absence of all coded characters	0
1	Appearance of: Scar for medial tibioastragalar ligament (2) Scar for <i>M. interosseus cruris</i> (3) Scar for internal lateral ligament (4) Assemblage of scars for <i>M. tibialis caudalis</i> , <i>M. tibialis cranialis</i> , and femorotibial ligament (6)	33
2	Appearance of: Ridge for <i>M. tibialis cranialis</i> extending from <i>M. flexor tibialis interior</i> scar (5)	67
3	Appearance of: Scars for femorotibial ligament and <i>M. tibialis caudalis</i> distinct from assemblage containing scar for <i>M. tibialis cranialis</i> (7)	100
Humerus		
0	Absence of all coded characters or characters defining subsequent stages	0
1	Appearance of: Scar for <i>M. teres major</i> and branch of <i>M. latissimus dorsi</i> (1) Scar for <i>M. humeroradialis</i> (3)	33
2	Appearance of: Scar for <i>M. anconaeus humeralis medialis</i> (4)	67
3	Appearance of: Scar for <i>M. scapulohumeralis profundus</i> (8)	100

2, 6 and 7. Cluster-based stage 1 is defined by the acquisition of characters 1 (scar for *M. teres major* and branch of *M. latissimus dorsi*) and 3 (scar for *M. humeroradialis*), and is equivalent to parsimony-based stage 1. Stages 2 and 3 are additional stages recognized by the cluster analysis. Stage 2 is defined by the appearance of character 4 (scar for *M. anconaeus humeralis medialis*), and stage 3 by the appearance of character 8 (scar for *M. scapulohumeralis profundus*).

Results of the parsimony analyses are of little utility for understanding the current sample. The only femora scored as less than fully mature represent documented hatchlings (ROM R6251, R6252, R6253), and all femora with lengths greater than 21 mm are scored

as 100% mature. Results for the tibia and humerus are similarly uninformative, with only two tibiae and three humeri falling below 100% mature. Of these, all humeri and one tibia are from hatchlings. This does not provide a useful size-independent estimate of skeletal maturity, because 97% of the femur sample, 93% of the tibiae and 94% of the humeri are unrealistically classified as 100% mature. For this reason the results of the parsimony analyses were not used in further examination of relationships between skeletal maturity and bone surface textures.

Results of the cluster analyses are more informative in that they allow separation of the sample into more realistic maturity levels (Table 4); however, certain ambiguities remain. Although in all cases visual

inspection of the graphs suggests some successive increase in the size at which subsequent maturity values appear (Fig. 5), most maturity levels encompass wide and overlapping size ranges. The exceptions are the 25% level for the femur and 0% level for the tibia and humerus that include only hatchlings, and the 33% level for the humerus that includes a restricted size range from 33 to 56 mm femoral length. In the femur, the 50% level occupies a wide range but is concentrated in the smaller half of the sample size range. In the tibia, visual inspection suggests a possible coarse progression from the 33% maturity level in the lower half of the range, through the 67% level occupying nearly the whole range, to the 100% level in the upper half.

There is no difference between the results and conclusions of the one-way fixed-effects ANOVA and of the Kruskal–Wallis ANOVA on Ranks. The ‘violation of the assumption of equal variances’ in the data set

Table 4. Number of individuals within cluster-based ontogenetic stages recognized for each element

Element	Ontogenetic stage	Percentage maturity	No. of individuals
Femur	0	0	0
	1	25	3
	2	50	21
	3	75	61
	4	100	24
Tibia	0	0	1
	1	33	16
	2	67	24
	3	100	4
Humerus	0	0	3
	1	33	7
	2	67	32
	3	100	6

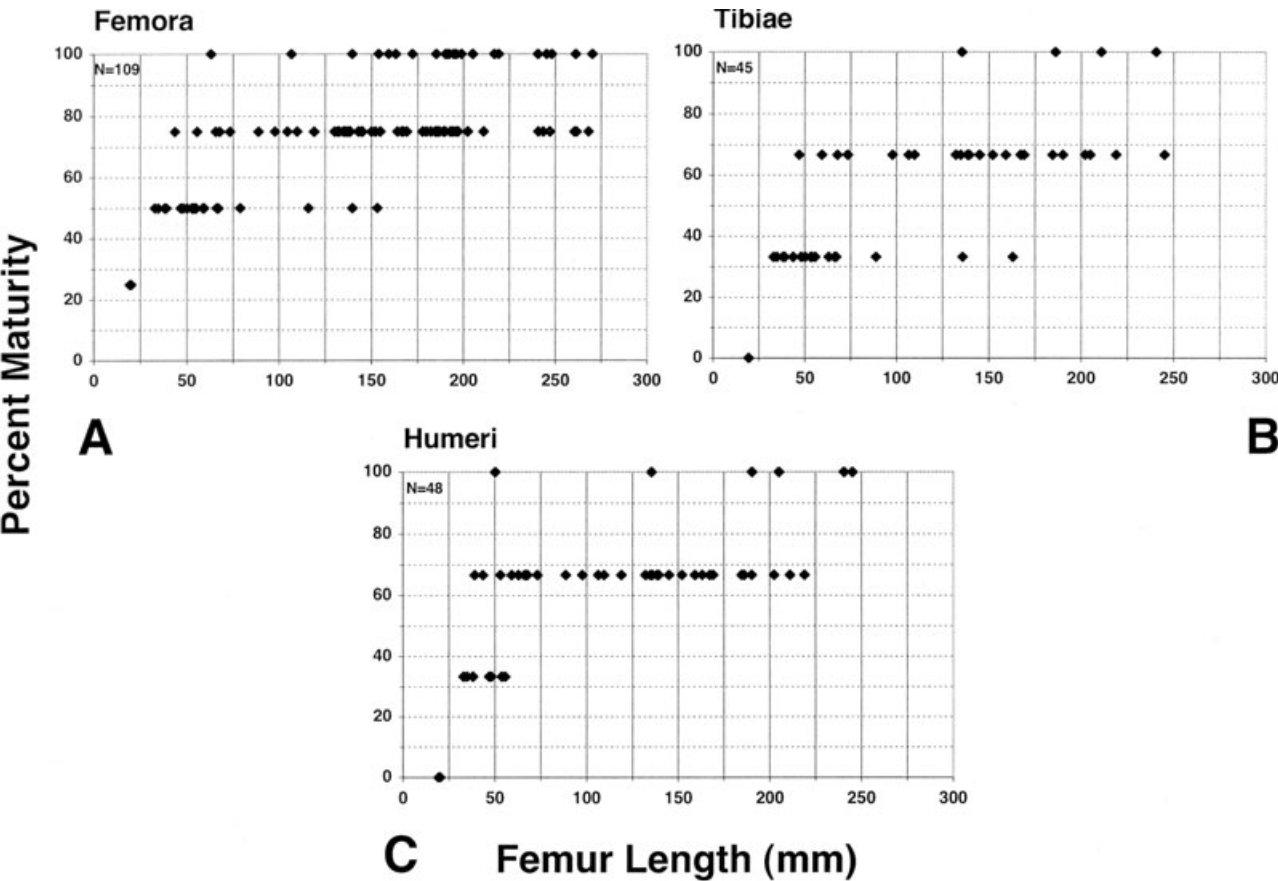


Figure 5. Relationships between femur length body-size proxy and element percentage maturity based on cluster analyses of long bone landmarks. A, femora: three individuals 25% mature, 21 individuals 50% mature, 61 individuals 75% mature, 24 individuals 100% mature. B, tibiae: one individual 0% mature, 16 individuals 33% mature, 24 individuals 67% mature, four individuals 100% mature. C, humeri: three individuals 0% mature, seven individuals 33% mature, 32 individuals 67% mature, six individuals 100% mature.

appears to be caused by sampling issues, rather than by a data distribution problem, and thus the regular ANOVA results may be considered to be accurate. The ANOVA model of the relationship between femur length and cluster-based ontogenetic stage is significant at $P < 0.01$. The post-hoc analysis via Tukey's test indicates that for the femur, stages 1 and 2 do not differ, but stages 3 and 4 are significantly different from each other as well as from stages 1 and 2. (No femora occupy stage 0.) Similarly, for the humerus, stages 0 and 1 do not significantly differ, but stage 2 and stage 3 are significantly different from each other as well as from stages 0 and 1. For the tibia, stages 0 and 1 are not significantly different, and nor are stages 2 and 3. The two sets (0 and 1, 2 and 3) are, however, different from each other. The significance values indicate that there does exist some basic relationship between ontogenetic stages as determined by cluster analysis and body size as determined by femur length; however, the situation is by no means clear-cut.

SURFACE TEXTURES

Seven major texture types are here defined for femora, tibiae and humeri of *Alligator mississippiensis*; these may be further divided into 12 subtypes. All texture types and subtypes occur in all elements. Types and subtypes with their numerical values are summarized in Table 5. It should be stressed that these textures are specific to *A. mississippiensis* and do not

correspond to the numbered texture types in our related study of the Canada goose *Branta canadensis* (Tumarkin-Deratzian *et al.*, 2006).

Persistent coarse surfaces

It should first be noted that in all individuals and on all elements, certain regions consistently retain a coarser pattern than surrounding surfaces. These areas are generally associated with muscle and/or ligament attachment sites, and are hereafter collectively termed persistent coarse surfaces (Fig. 6). On the femur, the fourth trochanter and surrounding attachments of *m. coccygeofemoralis longus* and *brevis* are rugose (Romer, 1923; Dodson, 1975; Brochu, 1996), marked by large open pits and pores (Fig. 6A). The proximal lateral (dorsal) surface of the bone is highly fibrous and marked by parallel ridges and furrows; this region includes the lateral attachment of *m. puboischiofemoralis internus pars dorsalis* and the proximal dorsal tuberosity (Brochu, 1996) (Fig. 6B). Similar ridges are found on the proximal cranial surface of the tibia, associated with attachment sites for *m. tibialis cranialis*, *m. flexor tibialis cranialis*, and the internal lateral ligament (Brochu, 1996). Rugose ridges are also found on the femoral and humeral condyles in areas of collateral ligament attachment (Fig. 6C) and on the distal cranial surface of the tibia at the attachment site of the medial tibioastragalar ligament. A roughened porous surface is often observed laterally

Table 5. Summary of texture types, subtypes, and assigned numerical values. Defining features of subtypes indicated by italics

Texture type	Defining features	Numerical value
I	Fuzzy fibrous pattern present	1.0
II	Etched porosity present; dotted porosity absent	
	<i>Porosity covers entire shaft</i>	2.0
	<i>Porosity fades out to proximal and distal smooth areas</i>	2.5
III	Co-occurrence of etched and dotted porosity	
	<i>Porosity covers entire shaft</i>	3.0
	<i>Porosity fades out to smooth proximal and distal areas</i>	3.3
	<i>Porosity co-occurs with large midshaft smooth areas</i>	3.7
IV	Dotted porosity present; etched porosity absent	
	<i>Porosity covers entire shaft</i>	4.0
	<i>Porosity fades out to smooth proximal and distal areas</i>	4.3
	<i>Porosity co-occurs with large midshaft smooth areas</i>	4.7
V	Shaft grossly smooth or faintly dimpled; Persistent coarse surfaces normal	5.0
VI	Shaft with scattered dotted porosity; Persistent coarse surfaces muted	6.0
VII	Shaft grossly smooth or faintly dimpled; Persistent coarse surfaces muted	7.0

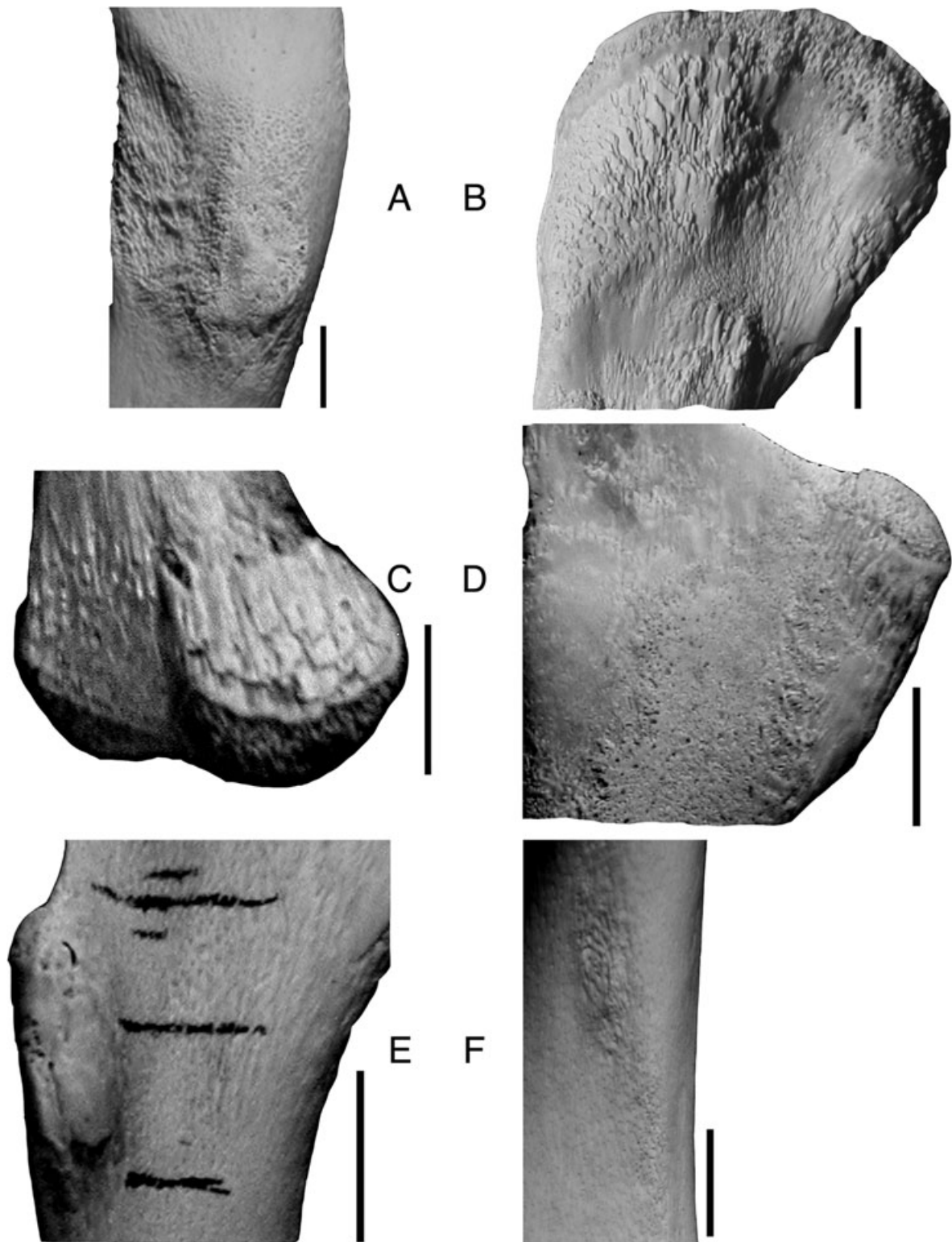


Figure 6. Examples of persistent coarse surfaces. A, femoral fourth trochanter in caudomedial (caudoventral) view (FWC LGS2). B, femoral proximal lateral (dorsal) surface (FWC LGS1). C, humeral medial (caudal) condyle in caudomedial (dorsocaudal) view, collateral ligament attachment site (FWC 35119). D, humeral deltopectoral crest, lateral (cranial) surface (FWC LGS3). E, humeral deltopectoral crest, craniomedial (ventrocaudal) surface (FWC 35119). F, adductor ridges on caudal surface of femoral shaft (FWC LGS2). Proximal is toward the top in all images. Scale bars = 1 cm.

(cranially) on the deltopectoral crest of the humerus at the insertion of *m. deltoideus clavicularis* (Meers, 1999, 2003) (Fig. 6D). A radiating fibrous and porous pattern occurs on the proximal medial (ventral) surface of the femur, as well as the medial (caudal) face of the deltopectoral crest and adjacent proximal cranial (ventral) surface of the humerus at the insertion of *m. coracobrachialis* (Brochu, 1996; Meers, 1999, 2003) (Fig. 6E). Finally, longitudinal ridges for attachment of the adductor musculature and *m. iliofemoralis* on the femur (Romer, 1923; Brochu, 1996), and *m. humero-radialis*, *mm. anconaeus humeralis caudalis* and *medialis* (Brochu, 1996) [*mm. triceps brevis cranialis* and *intermedius* of Meers (1999, 2003)] on the humerus often retain distinct porosity when surrounding regions are smoother (Fig. 6F).

Type I

Type I bones are characterized by a 'fuzzy fibrous' pattern covering nearly the entire shaft. Surfaces may or may not exhibit distinctly visible pores, but are markedly grainy and rough to the touch (Fig. 7A, B).

Type II

Type II bones exhibit 'etched porosity'. Visible pores penetrate the bone surface at variable angles and are often connected via shallow surface grooves, resulting in a disorganized, etched appearance mid-shaft (Fig. 7C, D). Greater organization may occur in more proximal and distal regions, with pores piercing the surface on an angle to form fibrous areas radiating toward the bone ends (Fig. 7E). Type II bones may be divided into two subtypes: in subtype 2.0 the porosity extends over the entire shaft; in subtype 2.5 porosity gradually fades out to be replaced by smooth areas proximally and distally.

Type III

Type III bones are characterized by co-occurrence of etched porosity and 'dotted porosity', a more organized porous pattern in which pores penetrate the bone surface at roughly right angles to the shaft (Fig. 7F). The two types of porosity may either occur independently on distinct areas of the bone, or overprint each other in the same region (Fig. 7G, H). As on type II bones, the angle of the pores may change along the shaft to create radiating fibrous regions proximally and distally. Three subtypes may be recognized: in subtype 3.0 porosity covers the entire shaft; in subtype 3.3 porosity fades out into smooth areas proximally and distally; and in subtype 3.7 porosity shares the midshaft region with large smooth areas in variable locations.

Type IV

Type IV bones exhibit dotted porosity but lack etched porosity. As with types II and III, radiating fibrous areas may occur proximally and distally. Three subtypes occur (4.0, 4.3, 4.7); these are defined by the same relative distributions of porous and smooth areas as the subtypes for type III.

Type V

Type V bones are grossly smooth, except on the persistent coarse surfaces described above. Faint, shallow dimples may occur in some areas, but these are not associated with pores that penetrate the bone surface (Fig. 8A, B).

Type VI

Type VI bones show a 'muted' pattern on persistently coarse surfaces. Ridges, furrows and shallow pits are still present, but are not as well defined as in previous textural types, and are generally not associated with penetrating pores (Fig. 8C, D). The rest of the shaft shows dotted porosity, but with the pores more widely scattered than in the dotted areas of types III and IV.

Type VII

Type VII bones occupy the least porous position on the texture spectrum, combining the smoothest features of types V and VI. Type VII bones are characterized by co-occurrence of a grossly smooth or faintly dimpled shaft with muting of textures and loss of porosity on persistently coarse surfaces.

RELATIONSHIP OF SURFACE TEXTURES TO SKELETAL MATURITY

When the relationship between texture type and body size based on femur length is examined (Fig. 9), texture type I is seen to be restricted to animals with femur length less than 68 mm. Within the femur subsample, type II appears restricted to this range as well, although type II texture also occurs on humeri and tibiae of individuals with femur lengths up to 119 mm and 190 mm, respectively. There is no clear difference in distribution of subtypes within texture types II–IV. Individuals of the largest size classes (femur length greater than 240 mm) appear restricted to texture types IV–VII; this corresponds to a complete absence of the fuzzy fibrous and etched porous textures. When only the femur is considered, types III and IV appear to perhaps represent successive stages, with the co-occurrence of etched and dotted porosity (type III) eventually giving way to dotted porosity alone (type IV). The amount of overlap between the

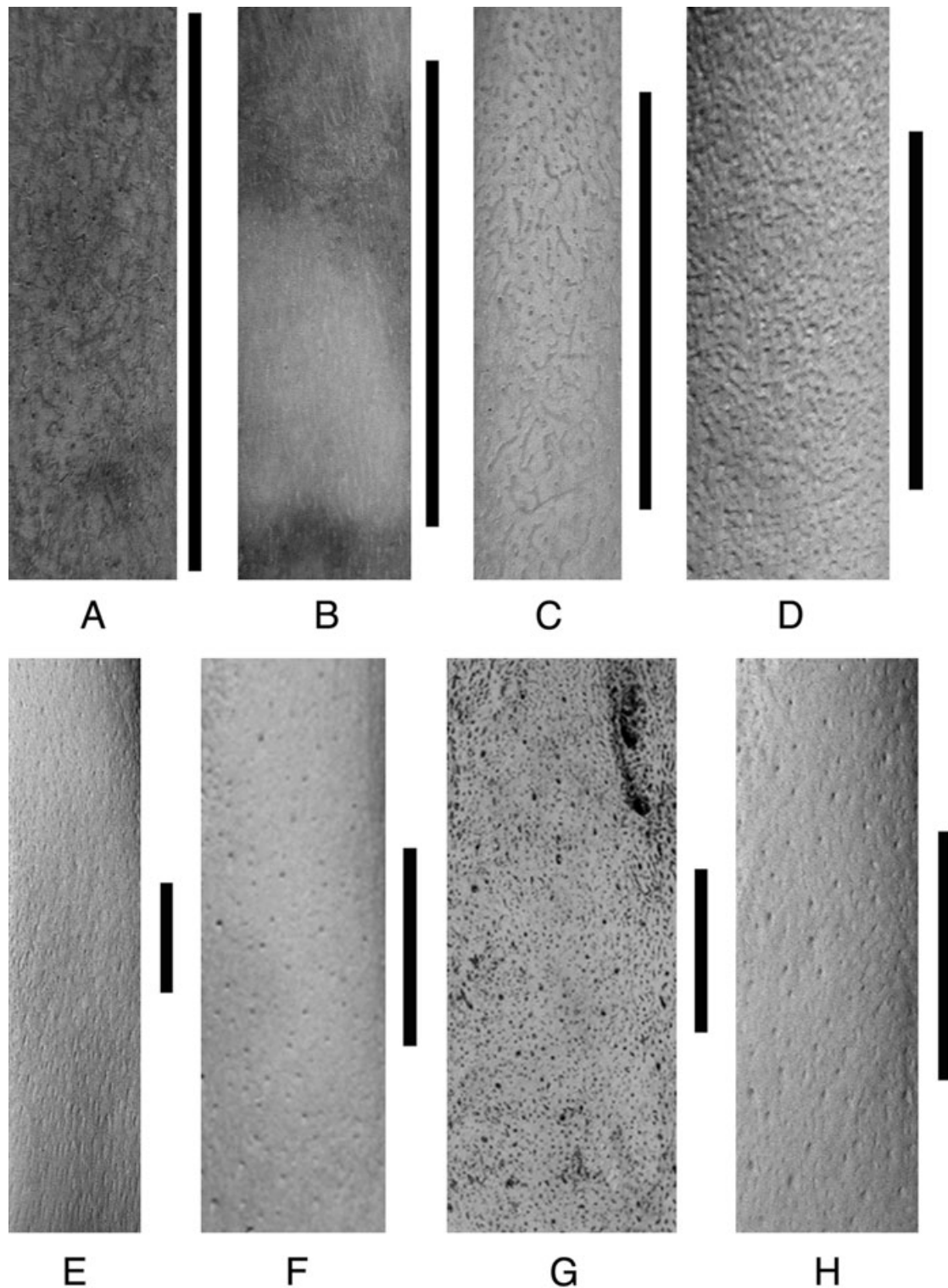


Figure 7. Examples of porous surface patterns. A, fuzzy fibrous pattern with visible pores (UF 109039, femur). B, fuzzy fibrous pattern without visible pores (UF 109039, humerus). C, etched porosity with connecting surface grooves (UF 38974, femur). D, etched porosity (FWC 35119, humerus). E, porous surface (top) grading into radiating fibrous surface (bottom) (FWC LGS1, femur). F, dotted porosity (FWC LGS2, femur). G, overprinted etched and dotted porosity, etched more prominent (ROM R4415, femur). H, overprinted etched and dotted porosity, dotted more prominent (FWC LGS1, femur). Scale bars = 1 cm.

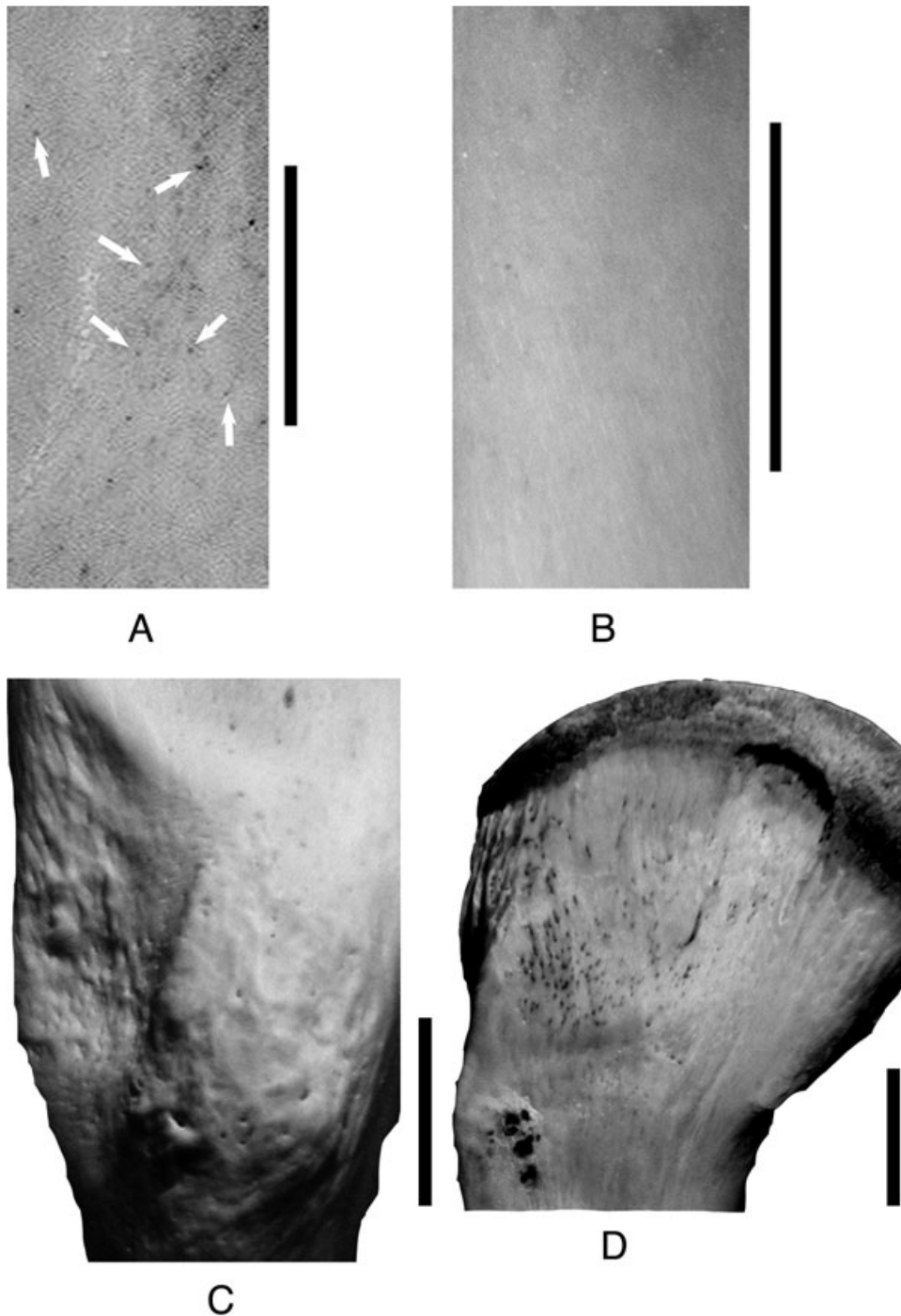


Figure 8. Examples of grossly smooth and muted persistent coarse surfaces. A, shallow surface dimples (arrows) (MOR HIP2001-08R-32, femur). B, smooth surface (FWC 40853, femur). C, muted texture, femoral fourth trochanter (FWC 40853). D, muted texture, femoral proximal lateral (dorsal) surface (FWC 40859). Scale bars = 1 cm.

two fields is, however, considerable, and this pattern is absent from the tibia and humerus subsamples. The wide range of sizes over which types II–VII occur makes them of extremely limited utility for estimating ages of isolated bones.

In the ANOVA model of the relationship between texture type and femur length, post-hoc analysis via Tukey's test indicates that the following relationships are statistically significant at $P < 0.05$. For the femur and humerus, texture types I and II are significantly

different from types III–VII, but within each of these groups texture types are not significantly different from one another. For the tibia, there are no significant differences between texture types. As with the visual inspection of Figure 9, it does not seem possible overall to relate bone surface texture and body size, other than to say that hatchling and small juvenile-sized bones generally exhibit only texture types I or II, and larger bones may exhibit any texture type, but rarely texture type I.

A corollary of the examination of the relationship between texture type and body size is the assumption that size is related to chronological age, which may not always be the case. Discrepancies between size and age have been documented in *Alligator mississippiensis* as a result of differences in relative growth rates of males and females and animals from different localities (McIlhenny, 1935; Peabody, 1961; Bellairs, 1970; Neill, 1971; Chabreck & Joanen, 1979; Andrews, 1982; Jacobsen & Kushlan, 1989; Magnusson *et al.*, 1989; Castanet *et al.*, 1993; Woodward *et al.*, 1995; Dalrymple, 1996; Wilkinson & Rhodes, 1997). Growth and size variations between wild and captive animals may also

be a confounding factor, as may variation caused by seasonal periods of slowed or arrested growth.

Restricting the size-based analysis to individuals of known sex (Fig. 10) does little to reduce the high variability of texture type distributions. Examination of Figure 10 does little more than confirm that males of *Alligator mississippiensis* reach a larger adult size than females. Texture types II–VII still occupy wide overlapping size ranges in both sexes.

Factoring season of death into the analysis also lends no additional resolution to the data set. One might argue that this reflects the fact that individuals dying during the transitional and inactive seasons comprise a limited portion of the total sample (five and six individuals, respectively). It is notable, however, that the individuals dying during the active season occupy the full range of textural variation seen in the total sample. Individuals dying during the transitional months of April and October are confined to texture types II and III in the femur and humerus subsamples, and types II–IV in the tibia subsample. This is, however, well within the distribution of active-season individuals at the same size ranges.

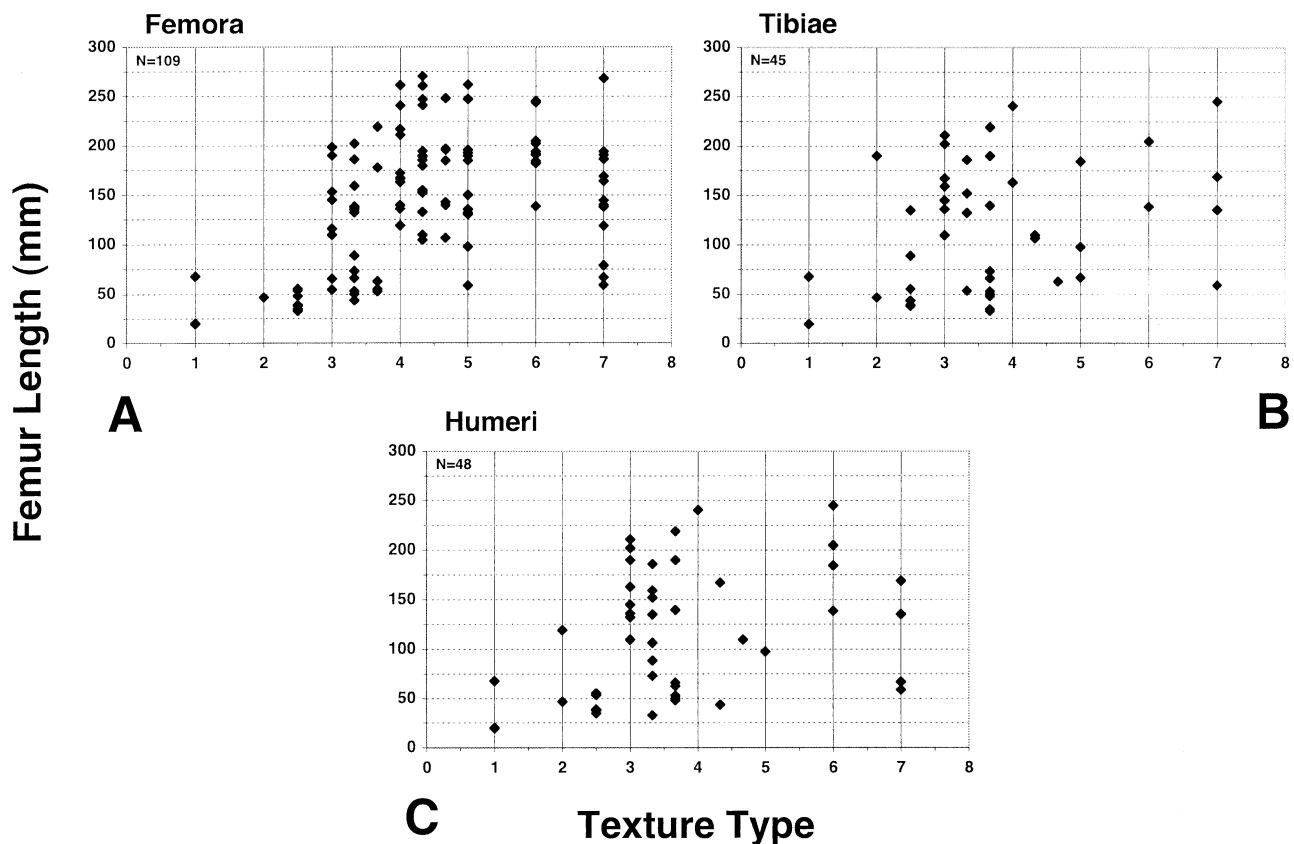


Figure 9. Relationship between bone texture type and femur length body-size proxy for all elements. A, femora. B, tibiae. C, humeri.

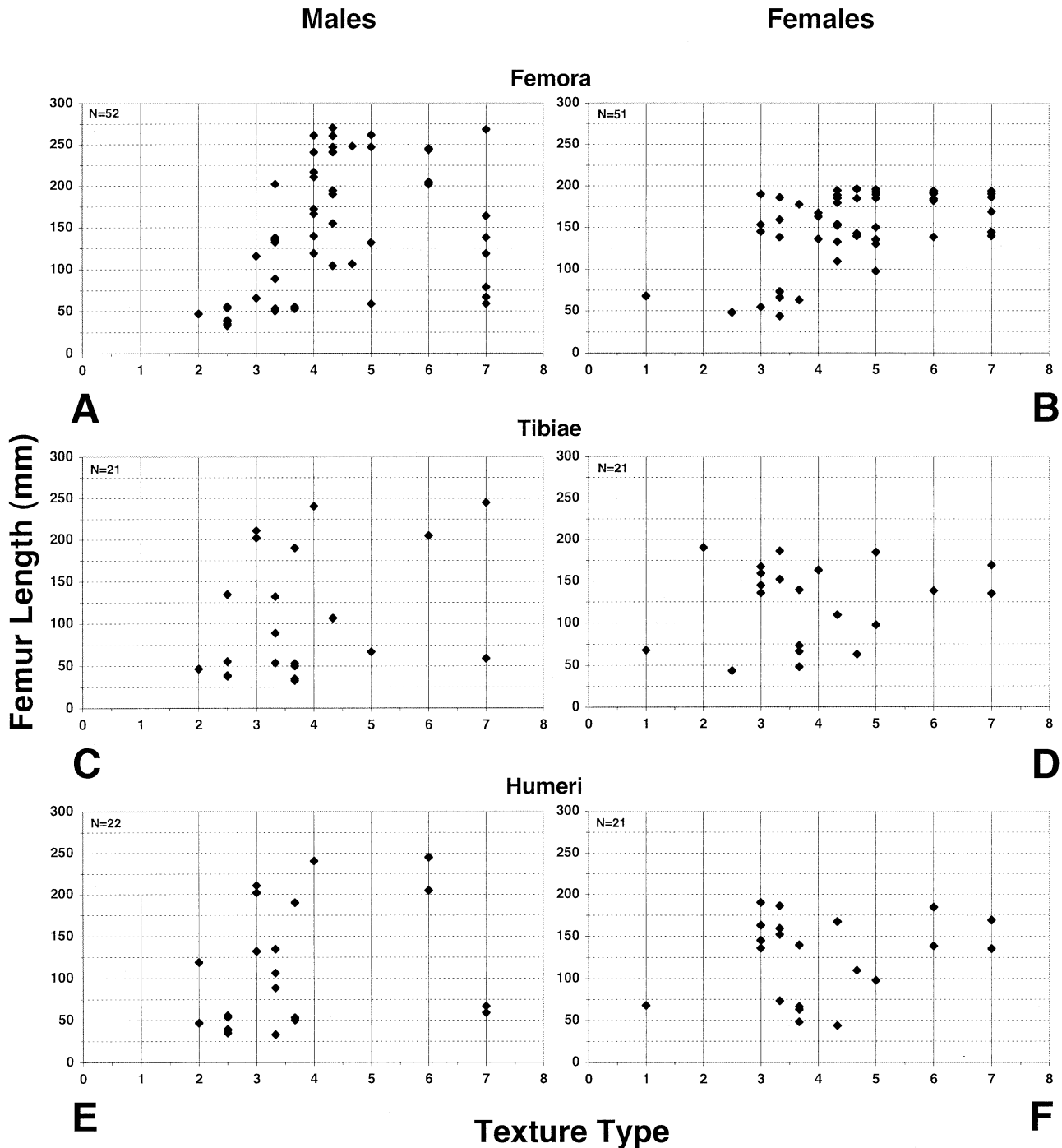


Figure 10. Relationships between bone texture type and femur length body-size proxy for individuals of known sex. A, male femora. B, female femora. C, male tibiae. D, female tibiae. E, male humeri. F, female humeri.

Although captive individuals account for the largest individuals in the study sample, the distribution of texture types is similar to that in the smaller wild individuals (Fig. 11). Thus, removal of the captive animals from the sample would do little to reduce variability of texture with respect to size. Farm-raised

individuals all exhibit texture types II–IV; however, this distribution is consistent with that of wild individuals of similar size.

Geographical variation in growth rates, combined with sexual dimorphism, may account for some of the variability observed in the femur length vs. texture

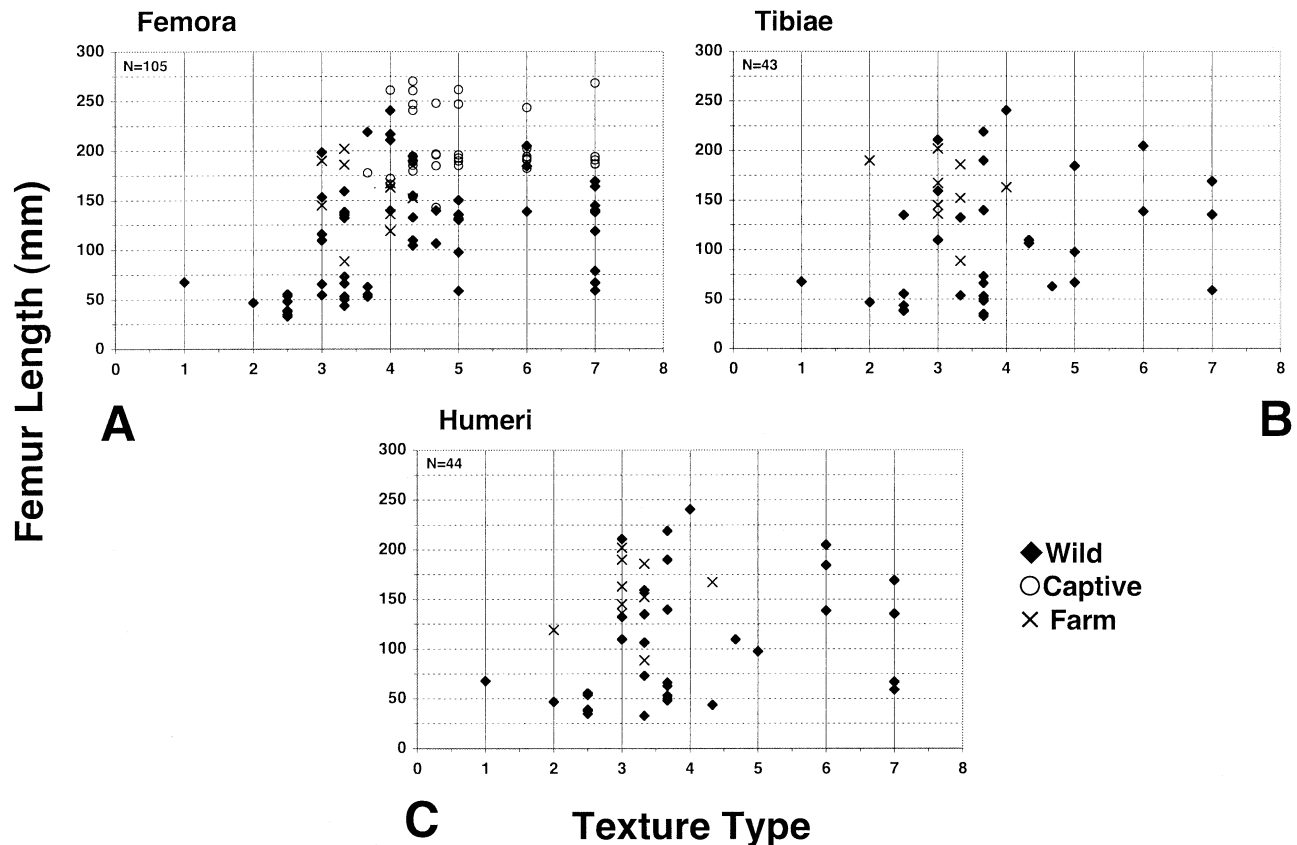


Figure 11. Relationships between bone texture type and femur length body-size proxy for individuals with known habitat. A, femora. B, tibiae. C, humeri.

plots. The total study sample includes individuals from Florida, Louisiana and South Carolina. The South Carolina subsample contains only three individuals, all hatchlings, and is excluded from the geographical analysis. Separate analysis of wild Louisiana individuals for the tibia and humerus is similarly of little utility due to the small sample size ($N = 8$). The Louisiana femur subsample shows no distinction between males and females. Texture type II is restricted to animals with femur length less than 54 mm, and, with the exception of one female with texture type III at 44 mm, is the only texture type present in individuals of femur length under 100 mm. Above this size range the other types show no distinct distribution. Plots of wild individuals from Florida, however, yield a potentially interesting result (Fig. 12). Although distribution of textural types among males remains variable for all three elements, there does appear to be a trend among females for a decrease in femoral surface porosity with increasing size. This trend is, however, weaker in the humerus and nearly absent in the tibia when the complete Florida subsample is considered. Previous studies have reported that growth in Everglades alligators tends to be retarded

relative to animals from elsewhere in Florida (Jacobson & Kushlan, 1989; Dalrymple, 1996). When tibial and humeral data for individuals from Everglades populations are separated out, the trend is again clearly visible among the females, although it remains absent among the males.

Use of the cluster-based ontogenetic stages (Fig. 13) provides little additional resolution beyond that obtained with the size-based plots. For the femur, texture type I occurs largely at the 25% maturity level, with one unusual individual retaining this texture at 75% maturity. Texture types III–V and VII occur from 50 to 100% maturity; type II occurs at the 50 and 75% levels; and type VI at 75 and 100%. In the tibia and humerus, type I is confined to the 0% level, and types VI and VII (both with muted regions of persistent coarse texture) occur only at 67 and 100% maturity. The humerus plot suggests a possible progression from texture types I and II (fuzzy fibrous and etched porosity) at 67% and below, to type III (both etched and dotted porosity) throughout the 33–100% range, to types IV–VII (dotted porous or smooth shaft with either normal or muted persistent coarse surfaces) at the 67 and 100% levels only. There is, however, con-

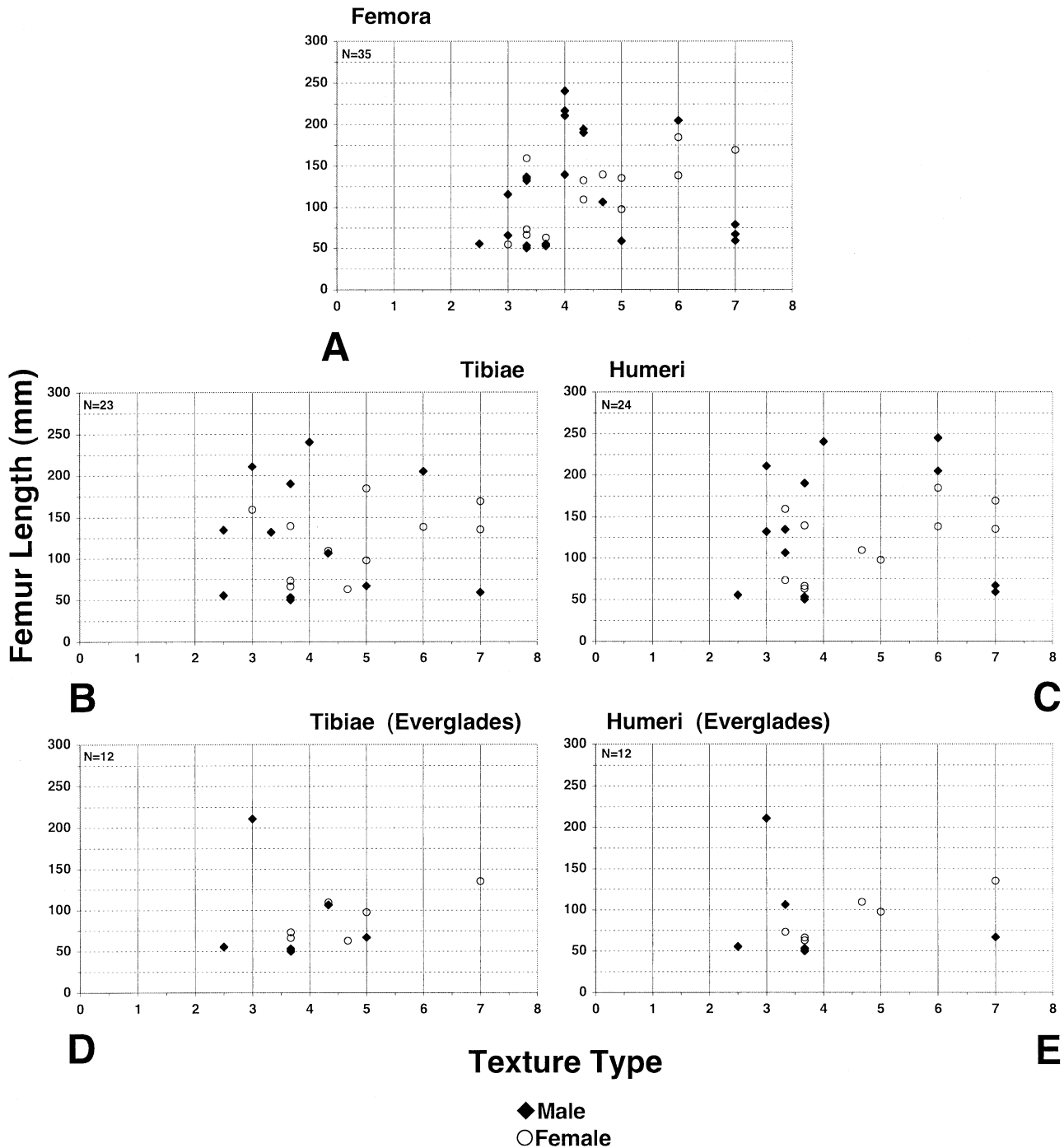


Figure 12. Possible geographical effect on the relationships between bone texture type and femur length body-size proxy for wild individuals of known sex. A, femora of Florida animals. B, tibiae of Florida animals. C, humeri of Florida animals. D, tibiae of Everglades animals only. E, humeri of Everglades animals only.

siderable overlap between fields. Moreover, none of the relationships suggested in the tibia and humerus is resolved in the femur, which is known from more than double the sample size of the other two elements. This raises the question of whether the relationships

would still exist in larger samples of tibiae and humeri.

Results of the statistical analyses of the two-way ranked-order contingency table to evaluate the relationship between texture type and cluster-based onto-

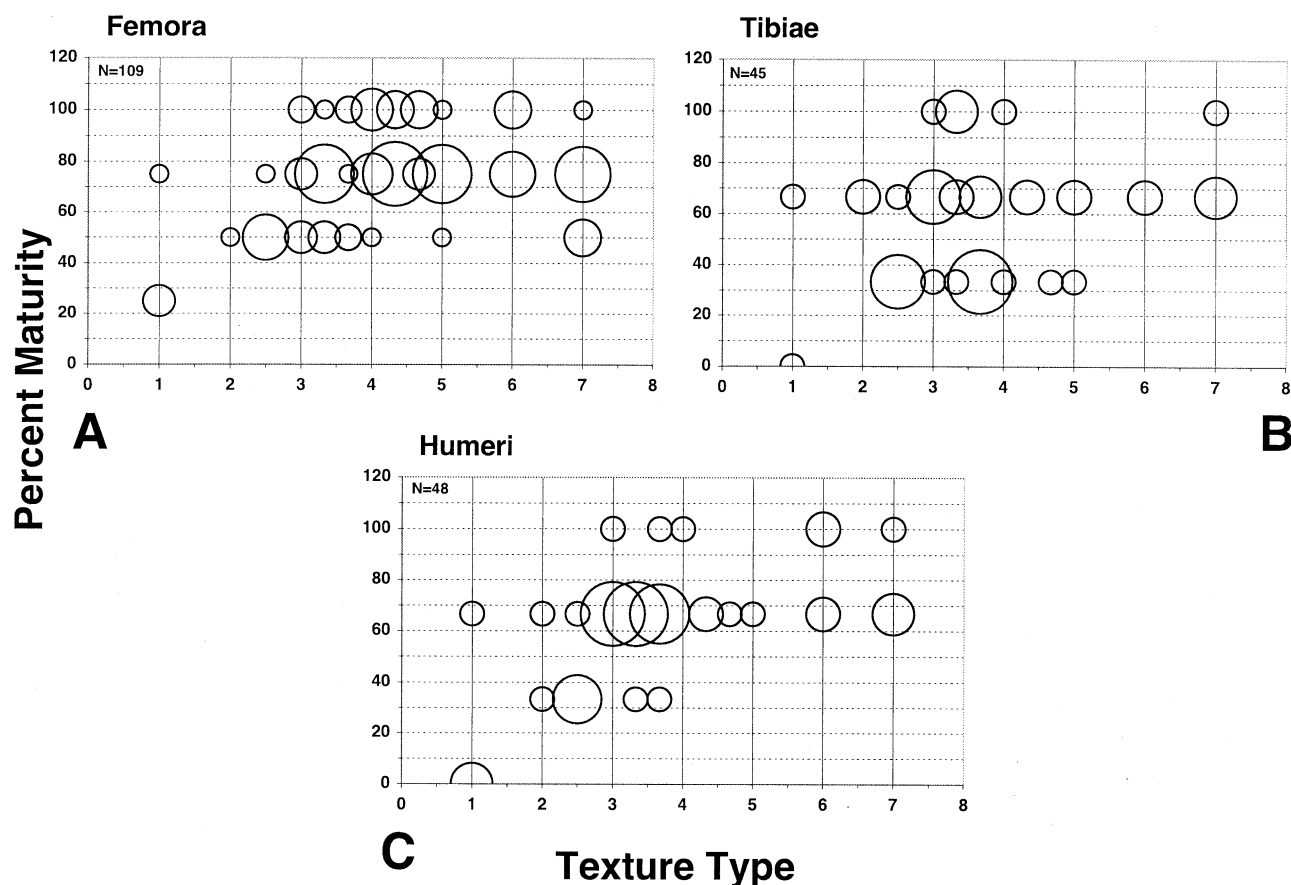


Figure 13. Relationships between bone texture type and cluster-based percentage maturity indices. Circle diameter proportional to number of individuals. A, femora: three individuals 25% mature, 21 individuals 50% mature, 61 individuals 75% mature, 24 individuals 100% mature. B, tibiae: one individual 0% mature, 16 individuals 33% mature, 24 individuals 67% mature, four individuals 100% mature. C, humeri: three individuals 0% mature, seven individuals 33% mature, 32 individuals 67% mature, six individuals 100% mature.

genetic stage are shown in Table 6. The chi-square (χ^2) values indicate that the two variables are not completely independent. This appears to be driven by the fact that texture type I occurs consistently as the only texture on bones of the lowest ontogenetic stages, and is also consistently absent from the most mature bones. The values for rho (ρ) and gamma (γ) are generally low, with large standard errors. The values for the humerus are closer to 1.0 than those for the femur and tibia, but again the error terms are quite high. The rho and gamma values indicate an overall weak association between ontogenetic stage and texture type, and suggest that knowledge of ontogenetic stage is not generally useful for predicting texture type, and vice versa, except in the case of hatchling individuals.

VARIATION WITHIN THE SKELETON

Of the 109 individuals examined, 61 are known from femora only. Of the 48 individuals for which more than

one element was available, 54% exhibit the same textural type on all elements examined, and 46% have elements of different textural types. In most of these cases, texture types correspond on two out of three elements. In only two individuals (UF 35150 and UF 37231) for which all three elements were examined is a different texture type documented on each element. As with comparisons of the same element among individuals, there does not appear to be any consistent pattern to the distribution of texture types on bones of the same individual.

HISTOLOGICAL CORRELATES OF SURFACE PATTERNS

No examples of the fuzzy fibrous pattern were present in the FWC sample available for thin sectioning. The presence or absence of the other porous patterns is for the most part correlated with the presence or absence of vascular channels intersecting the bone surface. Etched porosity is generally associated with zones

Table 6. Results of statistical analyses of the relationship between texture type and cluster-based ontogenetic stage

Element	Statistic	Coefficient	Asymptotic error	d.f.	P
Femur	χ^2	124.44		18	<0.005
	ρ	0.28	± 0.09		
	γ	0.32	± 0.12		
Tibia	χ^2	31.07		18	<0.03
	ρ	0.35	± 0.12		
	γ	0.46	± 0.16		
Humerus	χ^2	60.18		18	<0.005
	ρ	0.625	± 0.09		
	γ	0.745	± 0.095		

composed of fibrolamellar bone in which numerous channels penetrate the bone surface in variably longitudinal, oblique and circular orientations (Fig. 14A). The additional occurrence of large radial channels characterizes regions of overprinted etched and dotted porosity (Fig. 14B). The radiating fibrous pattern often encountered distally on porous bones appears to be related to an increasingly organized arrangement of primarily oblique to longitudinal channels in these regions (Fig. 14C).

In the absence of etched porosity, dotted porosity may be underlain by channels in any orientation. As when it overprints etched porosity, it is often associated with radial channels in fibrolamellar zones, but it may be underlain by oblique and longitudinal channels as well (Fig. 14D). In some instances, dotted porosity may also be associated with longitudinal channels in zones composed of lamellar bone (Fig. 14E).

Non-porous dimpled and smooth surfaces correspond to a lack or near lack of channels penetrating the bone surface. The dimpled pattern may be associated with a slightly undulating surface contour in thin section (Fig. 15A). Smooth surfaces occur with two underlying histological patterns. The first is a zone of lamellar bone sparsely vascularized with longitudinal channels that only rarely intersect the bone surface (Fig. 15B). A smooth surface may also occur when the periosteum is directly underlain by an annulus (Fig. 15C).

Persistent coarse surfaces exhibit histological patterns markedly distinct from other areas of the bone shaft. In many cases, Sharpey's fibres may be identified in these regions, confirming an association with areas of muscle and/or ligament attachment (Fig. 16A). The distal collateral ligament attachment sites on the femur and humerus are characterized in

thin section by irregular crenulated outlines combined with large longitudinal and oblique channels intersecting the bone surface (Fig. 16B). Similar architecture is often associated with the proximal lateral (dorsal) surface of the femur and the medial (caudal) surface of the deltopectoral crest. The femoral fourth trochanter and adjacent attachment of m. puboischiofemoralis bear an irregular filigree structure with large open channels that mirrors the grossly visible surface pattern (Fig. 16C, D). Active bone deposition is often seen in the form of partially roofed surface channels in these regions (Fig. 16C). Persistent coarse surfaces on the tibia, the proximal medial (ventral) surface of the femur, and the lateral (cranial) aspect of the deltopectoral crest exhibit surface incorporation of longitudinal channels. These are generally larger and more closely spaced than longitudinal channels occurring elsewhere in the bone shaft (Fig. 16E). This pattern may also occur on the medial (caudal) surface of the deltopectoral crest and adjacent proximal cranial (ventral) humeral surface (Fig. 16F).

Muted patterns on persistently coarse surfaces are grossly associated with a loss of porosity. As in other areas of the shaft, this is visible histologically as a loss of intersections of channels with the bone surface, although irregular or crenulated surface contours are retained (Fig. 17). In some regions, most notably the femoral fourth trochanter, the open filigree structure still persists at depth, but the surface bone is largely uninterrupted by these deeper channels (Fig. 17B).

DISCUSSION

There is no good correspondence between texture type and body size in *Alligator mississippiensis* (Fig. 9). Body size in *A. mississippiensis* may, however, be decoupled from chronological age and skeletal maturity due to a number of factors, including sexual dimorphism, seasonally interrupted growth, and various environmental conditions such as habitat, temperature and diet (McIlhenny, 1935; Peabody, 1961; Bellairs, 1970; Neill, 1971; Chabreck & Joanen, 1979; Andrews, 1982; Jacobsen & Kushlan, 1989; Magnusson *et al.*, 1989; Elsey *et al.*, 1990; Rootes *et al.*, 1991; Castanet *et al.*, 1993; Woodward *et al.*, 1995; Dalrymple, 1996; Wilkinson & Rhodes, 1997; Elsey *et al.*, 2000a, b; Lance *et al.*, 2000; Richardson *et al.*, 2002). To every extent possible, effort was made to factor these variables into the size-based analyses of the study sample. No clear distribution of texture types emerges; however, certain variables such as diet and ambient habitat temperature were in most cases unknown and impossible to control for.

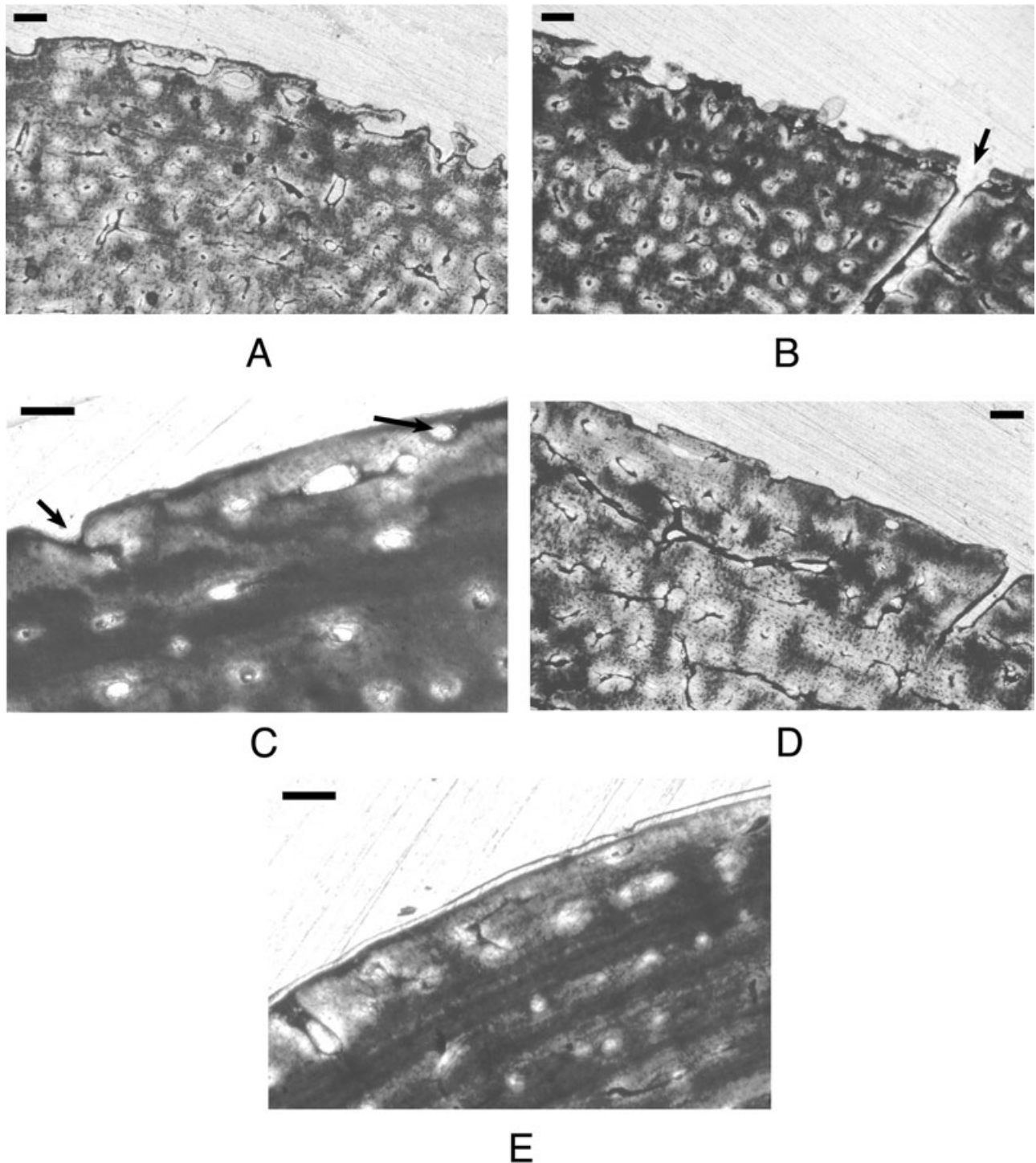


Figure 14. Histology underlying porous surface patterns. A, zone of fibrolamellar bone underlying etched porous surface (FWC 40723, tibia section c). B, fibrolamellar zone with large radial channels (arrow) underlying surface with overprinted dotted and etched porosity (FWC 40723, femur section c). C, longitudinal channels underlying radiating fibrous region, with arrows indicating channels intersecting and recently incorporated into the bone surface (FWC LGS4, femur section d). D, channels in varying orientations underlying dotted porous surface (FWC LGS1, femur section c). E, zone of lamellar bone underlying dotted porous surface (FWC 40583, humerus section c). Scale bars = 230 μm .

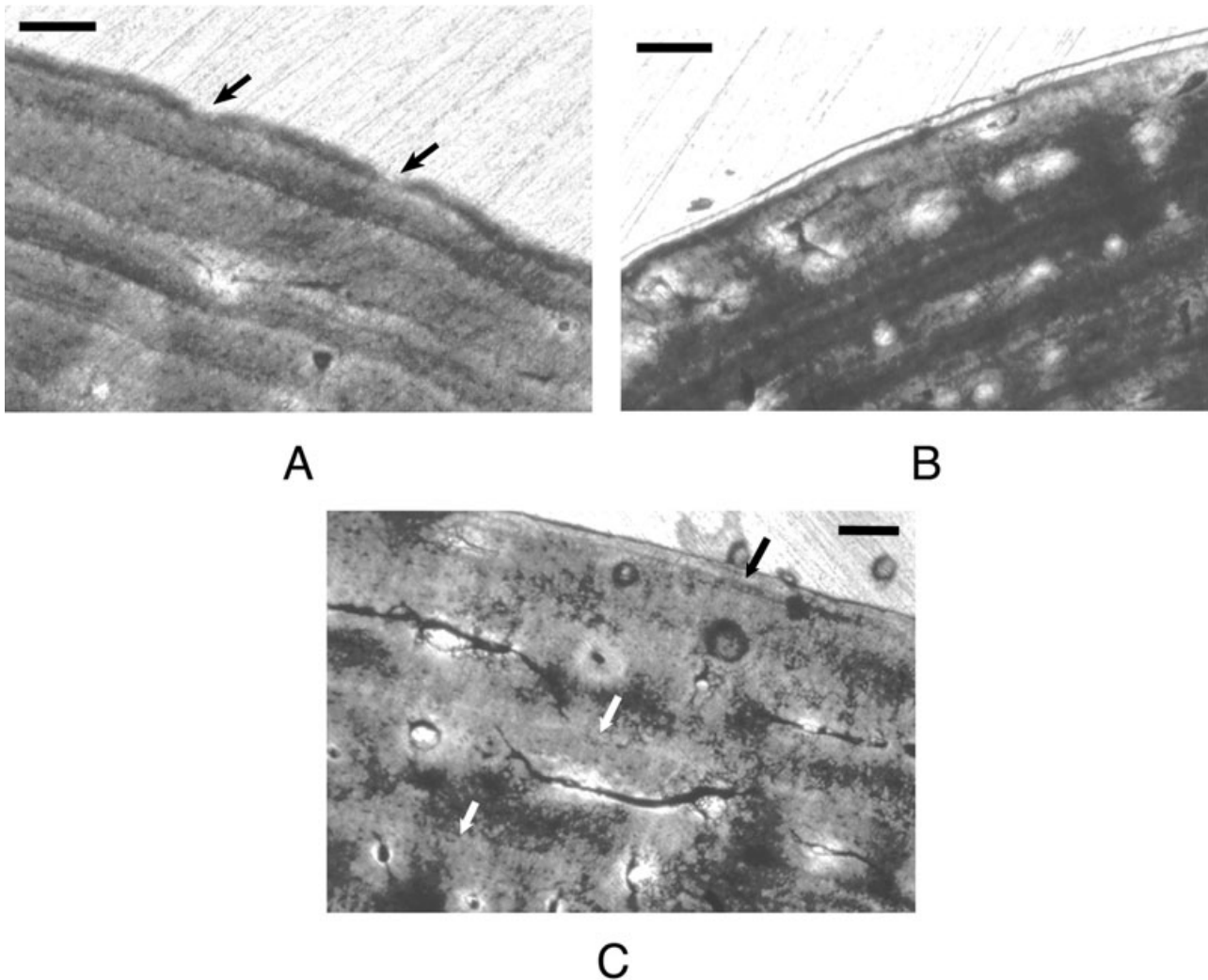


Figure 15. Histology underlying grossly smooth surface patterns. A, slight surface undulations (arrows) associated grossly with shallow dimples (FWC 40854, femur section b). B, smooth surface underlain by zone of lamellar bone (FWC 40583, humerus section c). C, smooth surface underlain by annulus. Arrows indicate annuli throughout cortex (FWC LGS8, tibia section d). Scale bars = 230 μ m.

SEXUAL DIMORPHISM

Previous studies of *Alligator mississippiensis* have reported larger adult sizes for males relative to females, as well as sexual dimorphism in growth rates, such that average growth rate in females decreases relative to that of males after a certain point in ontogeny (Bellairs, 1970; Neill, 1971; Chabreck & Joanen, 1979; Magnusson *et al.*, 1989; Woodward *et al.*, 1995; Wilkinson & Rhodes, 1997). Chabreck & Joanen (1979) report that in wild individuals from Louisiana, growth rates in both sexes are similar until roughly 3 years of age at length of approximately 1.0 m. Growth rates in males and females gradually begin to decrease after age 1 year. After age 3 years this

decline becomes progressively more pronounced in females such that male growth rates exceed those of females by nearly 20%. This percentage increases with age, with males growing 62% faster than females by age 10 years, 120% faster by age 15 years, and nearly 200% faster by age 20 years (Chabreck & Joanen, 1979). Sexually dimorphic growth rates may confound a size-based analysis of textural trends, due to the potential for lumping younger, faster growing males with older, more slowly growing females in the same size range. Accounting for sex in the study sample, however, has little effect on the distribution beyond confirming that males reach larger sizes than females. A high degree of textural variability with respect to body size is seen in both sexes (Fig. 10).

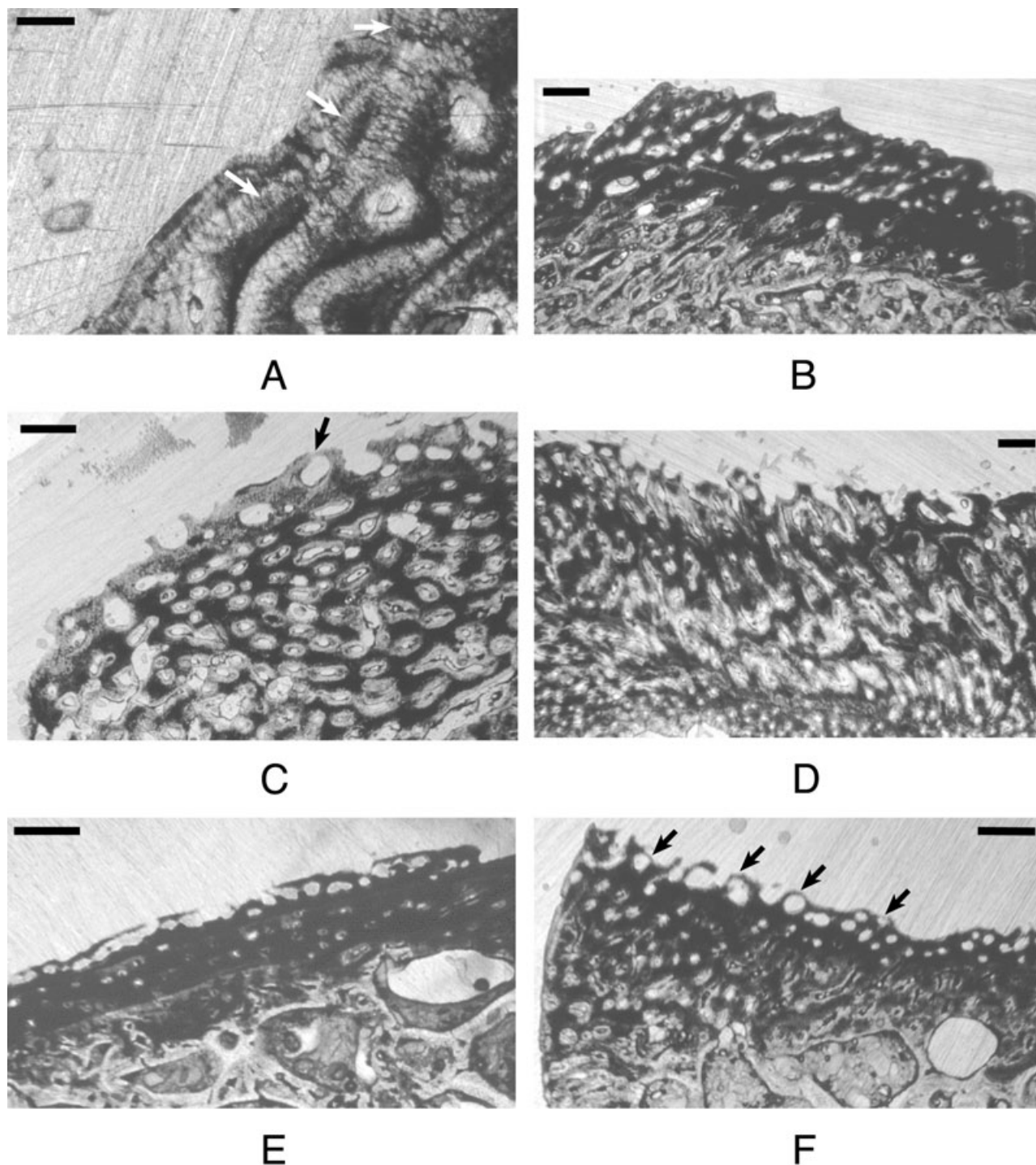


Figure 16. Histology of normal persistent coarse surfaces. A, Sharpey's fibres (arrows) visible as black thread-like structures beneath the bone surface (FWC LGS8, tibia section a). B, collateral ligament attachment site (FWC 40583, femur section e). C, fourth trochanter. Arrow indicates recently enclosed channel (FWC 40723, femur section b). D, attachment of m. puboischiofemoralis (FWC LGS1, femur section b). E, lateral (cranial) surface of deltopectoral crest (FWC 40723, humerus section b). F, humeral proximal cranial (ventral) surface. Arrows indicate recently enclosed channels (FWC 35119, humerus section a). Scale bars: A = 230 μ m; B–F = 919 μ m.

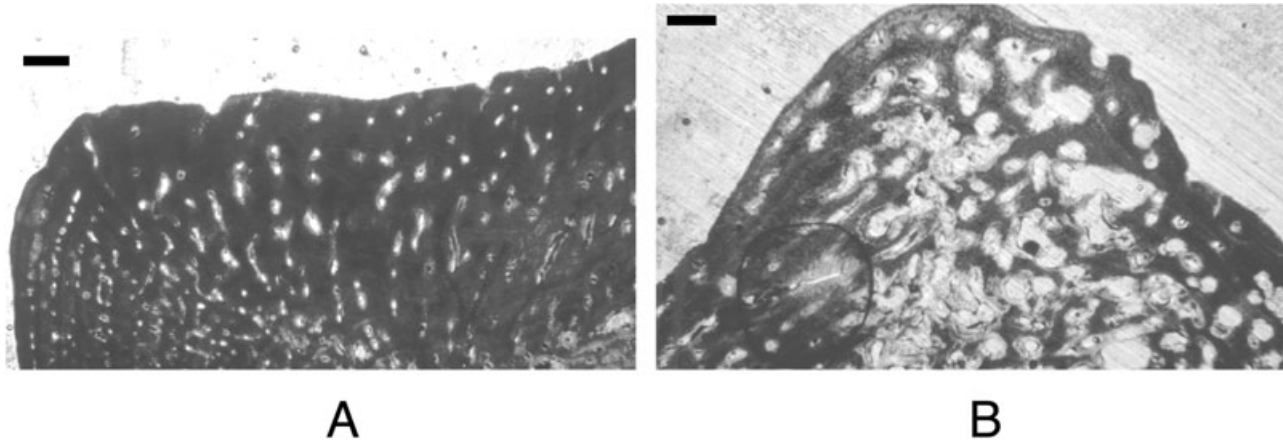


Figure 17. Histology of muted persistent coarse surfaces. A, attachment of m. puboischiofemoralis (FWC 40583, femur section b). B, fourth trochanter (FWC 40583, femur section b). Scale bars = 919 μm .

INTERRUPTED GROWTH

In the bone of wild crocodylians, seasonal variations in growth rate are visible histologically as zones and annuli and/or LAGs. These histological features have also been documented in captive crocodylians living under more-or-less constant conditions, although they may not be as pronounced as in wild individuals (e.g. de Buffrenil, 1980b). Since the immature textural types described in previous studies are associated with active osteological growth processes, it is reasonable to hypothesize that an individual dying during a period of slowed or arrested growth would not exhibit these textural features, regardless of overall skeletal maturity. Factoring season of death into the analysis, however, does nothing to resolve the variability in the texture type vs. size plots. The full range of variability is present in animals dying during the expected season of active growth (May–September). In theory it is possible that some individuals dying during the active season could have experienced slowed growth associated with undocumented illness or injury; however, formation of annuli and/or LAGs in response to stress has not previously been reported in modern crocodylians. Moreover, this does not explain the presence of porous surface patterns in animals dying during the transitional and inactive growth seasons.

HABITAT AND GEOGRAPHICAL RANGE

Alligators incubated and raised in captivity under optimum conditions of temperature, nutrition, etc., have shown the potential for higher sustained growth rates than wild individuals (e.g. de Buffrenil, 1980b; Elsey *et al.*, 2000a, b; Lance *et al.*, 2000). Elsey *et al.* (2000a) document accelerated growth in captive indi-

viduals incubated and raised at 30–32 °C. Accelerated growth in these individuals was maintained up to 4 years after release into the wild. It is also possible for captive animals to experience retarded growth relative to their wild counterparts if nutritional and temperature requirements are not met, or as a result of other stresses such as crowding (e.g. Elsey *et al.*, 1990; Lance *et al.*, 2000; Huchzermeyer, 2002). It is therefore a reasonable hypothesis that captive or farm-raised animals may show a different distribution of texture types than wild individuals. Farm-raised individuals in this study cluster together and all exhibit texture types II–IV; however, this does not differ from the distribution of wild individuals in the same size range (Fig. 11). It is impossible to tell from the data, however, whether or not some individuals coded as wild at time of death may have been previously released from captivity.

Previous studies of growth in *Alligator mississippiensis* conclude that growth rates vary throughout the species' geographical range due to local environmental conditions and resource availability (Jacobsen & Kushlan, 1989; Rootes *et al.*, 1991; Dalrymple, 1996; Wilkinson & Rhodes, 1997). It may therefore be fruitless to employ size as an age proxy for a sample drawn from multiple geographical areas. Geographical variation in growth rates, combined with sexual dimorphism, may account for some of the variability observed in the study sample (Fig. 12). Consideration of only Florida individuals reveals that although distribution of textural types among males remains variable, there may be a slight trend among females for a decrease in femoral surface porosity with an increase in body size. It may be that an earlier and greater slowing of growth in female individuals is responsible for the presence of a more consistent pattern in this

sex. The pattern is only resolved in the tibia and humerus subsamples when analysis is restricted to individuals from Everglades populations. This also suggests that texture type may be more tightly linked with size/age in slower growing individuals, as Everglades populations of *A. mississippiensis* have been shown to grow 3–4 times more slowly relative to populations elsewhere in Florida and Louisiana (Jacobsen & Kushlan, 1989; Dalrymple, 1996).

INDETERMINATE GROWTH

Although growth in *Alligator mississippiensis* is generally described as indeterminate, this does not mean that an individual continues growing at a constant rate throughout life. As noted above, growth rates in females decrease relative to those in males. Growth rates also appear eventually to decrease further in both sexes, becoming nearly asymptotic after total lengths of 2.5 and 3.5 m are attained in females and males, respectively (Woodward *et al.*, 1995; Wilkinson & Rhodes, 1997). One might expect that a prolonged period of growth may cause porosity to be highly persistent throughout ontogeny. Although this may explain the occurrence of relatively porous surfaces such as those of texture type III in larger and more mature individuals, it does little to account for the reverse phenomenon, i.e. the persistent occurrence of the low porosity of texture types V–VII in smaller and less mature individuals.

INDIVIDUAL VARIATION

Due to the failure of other factors to account fully for the high textural variability, one must by default hypothesize a high degree of individual variation in growth rates. Such variation could account for a decoupling in size vs. age, as well as for the occurrence of different textural types in animals of similar sizes and ages. This interpretation is supported by the fact that the high textural variability remains when the size-independent percentage maturity values derived from the cluster analyses are used as an age proxy.

Notable variation in growth rate occurs even among individuals of the same population. Individuals FWC 40723 and FWC 40583 are both from Lake Griffin, Florida, and are of comparable body size (snout–vent lengths of 99.5 and 100 cm, femur lengths of 134.77 and 139.48 mm, respectively). Limbs from these animals were obtained as frozen specimens from fresh-kill necropsies performed by FWC. Limbs were skeletonized at the same time by identical procedures, eliminating the possibility of variable taphonomic effects on bone surfaces. Femora from these two individuals exhibit markedly different textures (Fig. 18A, B). FWC 40723 has a highly porous texture (type III);

FWC 40583 is smoother with only faint scattered dotted porosity (type IV). Histologically, these bones bear evidence of completely different growth histories. FWC 40723 has wide zones composed of fibrolamellar bone with many vascular channels intersecting bone surfaces (Fig. 18C); application of skeletochronology yields a minimum age estimate of 5 years. FWC 40583 has narrower zones of lamellar bone with sparse longitudinal channels with few surface intersections (Fig. 18D); skeletochronology gives a minimum age estimate of 16 years. A significant difference between the two individuals is that FWC 40723 is male and FWC 40583 is female. One explanation of such differences in age and growth rate at comparable sizes is therefore sexual variation. The lack of resolution on the texture-type plots when sex is considered (Fig. 10), however, suggests the possible involvement of additional factors. Given that these individuals are drawn from the same population, individual variation in growth rates is a likely candidate, although the precise cause of such variation remains unknown.

CONCLUSIONS

The data presented here show little to no association between bone textures and either body size or skeletal maturity in *Alligator mississippiensis*. Indeterminate growth alone fails to account for all observed textural variation, particularly the occurrence of low-porosity surface patterns in individuals of smaller size and lower maturity classes. It seems likely that high sensitivity to local and regional environmental conditions, coupled with long periods of time to reach full adult size, renders growth in *A. mississippiensis* too variable to apply the textural ageing method successfully.

A related study on the Canada goose *Branta canadensis* using identical methodology (Tumarkin-Deratzian *et al.*, 2006) reveals an excellent correlation between textural types and skeletal maturity. In *B. canadensis*, distinct suites of textures readily distinguish juveniles, subadults and adults with little to no overlap between groups. It should be stressed that the surface patterns and texture types defined here for *Alligator mississippiensis* do not directly equate to those recognized in *B. canadensis*. Etched porosity and persistent coarse surfaces similar to those defined for *A. mississippiensis* are not present on *B. canadensis* long bones. Also, certain surface patterns characteristic of *B. canadensis* are absent in *A. mississippiensis*. This underlines the point that there does not seem to exist a universal system of surface textural patterns definable across taxa. If the textural ageing method is to be applied therefore textures must be to some degree taxon-specific.

The growth regime of *Branta canadensis* individuals, which undergo determinate growth and reach full

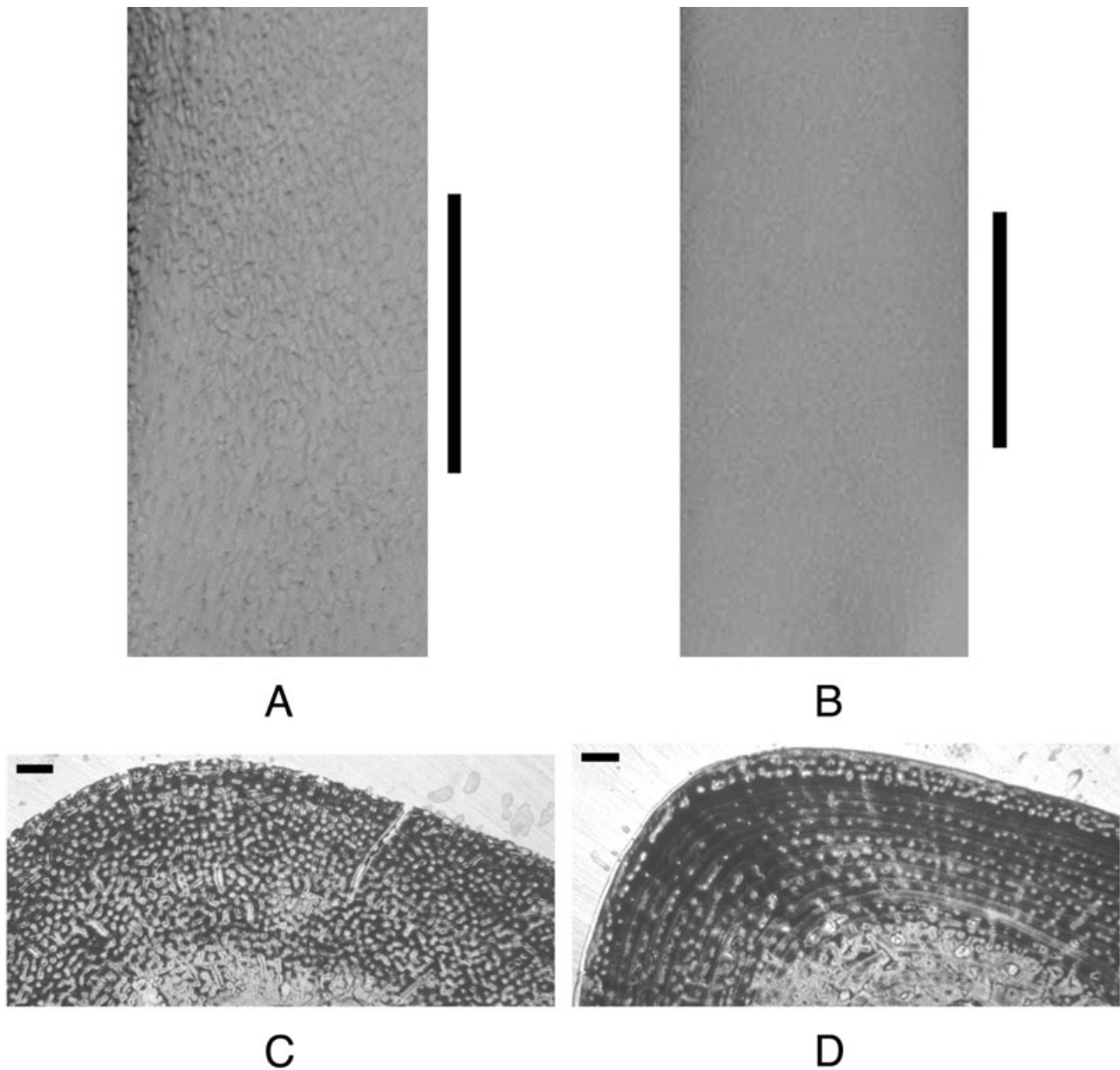


Figure 18. Individual variation in surface pattern and growth in Lake Griffin alligators. A, overprinted etched and dotted porosity (FWC 40723, femur). B, mainly smooth surface with faint scattered dotted porosity (FWC 40583, femur). C, fibro-lamellar zones underlying porous surface shown in A (FWC 40723, femur section c). D, lamellar zones underlying smooth surface shown in B (FWC 40583, femur section c). Scale bars: A, B = 1 cm; C, D = 919 μ m.

adult size within one 7-month growing season, is, of course, in strong contrast to the seasonally interrupted indeterminate growth of *Alligator mississippiensis*. This suggests that growth regime may be an important controlling factor in determining the reliability of the textural ageing method. The fact that season of death and indeterminate growth alone cannot account for the extreme variability in the *A. mississippiensis* sample, even when sex is controlled for, indicates that addi-

tional factors such as a high degree of individual variation are probably involved.

Histological analysis reveals that, as in *Branta canadensis*, bone surface patterns in *Alligator mississippiensis* are expressions of osteological growth processes. However, the histology of *A. mississippiensis* also reveals marked individual variation in growth pattern and rate. Given such variability in growth, it is probably of little utility that surface pattern corre-

lates with histology. Bone surface patterns may be potentially indicative of the animal's growth pattern at any given time, but are essentially useless for determining relative maturity of individuals.

Results of the *Alligator mississippiensis* study indicate that bone surface textures cannot be relied upon as universal indicators of skeletal maturity. Indeterminate interrupted growth regime may be one confounding factor, combined with a high degree of individual variation in growth rate and sensitivity to local conditions. These are probably linked; it is reasonable to assume more latitude for growth variation in a species such as *A. mississippiensis* with indeterminate growth compared with a rapidly maturing species with determinate growth such as *Branta canadensis*. Use of the textural ageing method for modern and fossil crocodylians is not recommended. Until such time as controlling factors are better understood, the application of the textural ageing method to fossil taxa with indeterminate growth regimes or for which growth regime is unknown should only be attempted with extreme caution and in cases where other means of estimating maturity are also available to provide corroboration.

ACKNOWLEDGEMENTS

The following individuals and institutions granted access to specimens under their care: F. Wayne King, J. Perran Ross and Kenneth Krysko (UF), Kevin Seymour and Hans-Dieter Sues (ROM), and Cynthia Marshall (MOR). James Farlow invited study of the MOR sample and provided access to unpublished body-size data for those animals. J. Perran Ross supervised salvage of Lake Griffin animals under the auspices of FWC and Special Use permit WXO1261; Allan Woodward granted use of FWC facilities for initial processing of salvaged material. Diane Borden-Billiot, Ruth Elsey and Grant Hurlburt provided locality and habitat data for many individuals from the MOR and UF samples. Chris Brochu supplied unpublished supplemental data on characters used in the parsimony analysis. David Deratzian provided technical assistance with photographic images. Chris Brochu, Tom Carr, Anusuya Chinsamy-Turan, Greg Erickson, James Farlow, Barbara Grandstaff, Fritz Huchzermeyer, Matthew Lamanna and J. Perran Ross provided much stimulating and informative discussion. Portions of this work were supported by the Geological Society of America, the Jurassic Foundation, the Paleontological Society, Sigma Xi, the University of Pennsylvania Summer Stipends in Paleontology program, a National Science Foundation Graduate Research Fellowship to Allison R. Tumarkin-Deratzian, and National Science Foundation Grant EAR 95-06694 to Peter Dodson.

REFERENCES

- Andrews RM. 1982.** Patterns of growth in reptiles. In: Gans C, Pough FH, eds. *Biology of the Reptilia*. Vol. 13, *Physiology D*. New York: Academic Press, 273–320.
- Bellairs A. 1970.** *The life of reptiles*, Vol. 2. New York: Universe Books.
- Benecke N. 1993.** On the utilization of the domestic fowl in central Europe from the Iron Age up to the Middle Ages. *Archaeofauna* **2**: 21–31.
- Bennett SC. 1993.** The ontogeny of *Pteranodon* and other pterosaurs. *Paleobiology* **19**: 92–106.
- Brill K, Carpenter K. 2001.** A baby ornithomimid from the Morrison Formation of Garden Park, Colorado. In: Tanke DH, Carpenter K, eds. *Mesozoic vertebrate life*. Bloomington: Indiana University Press, 197–205.
- Brinkman D. 1988.** Size-independent criteria for estimating relative age in *Ophiacodon* and *Dimetrodon* (Reptilia, Pelycosauria) from the Admiral and Lower Belle Plains Formations of west-central Texas. *Journal of Vertebrate Paleontology* **8**: 172–180.
- Brochu CA. 1992.** *Ontogeny of the postcranium in crocodylomorph archosaurs*. MA thesis, University of Texas at Austin.
- Brochu CA. 1996.** Closure of neurocentral sutures during crocodilian ontogeny: implications for maturity assessment in fossil archosaurs. *Journal of Vertebrate Paleontology*. **16**: 49–62.
- de Buffrenil V. 1980a.** Données préliminaires sur la structure des marques de croissance squelettiques chez les crocodiliens actuels et fossiles. *Bulletin de la Société Zoologique de France* **105**: 355–361.
- de Buffrenil V. 1980b.** Mise en évidence de l'incidence des conditions de milieu sur la croissance de *Crocodylus siamensis* (Schneider, 1801) et valeur des marques de croissance squelettiques pour l'évaluation de l'âge individuel. *Archives de Zoologie Expérimentale et Générale* **121**: 63–76.
- Callison G, Quimby HM. 1984.** Tiny dinosaurs: are they fully grown? *Journal of Vertebrate Paleontology* **3**: 200–209.
- Carr TD. 1999.** Craniofacial ontogeny in Tyrannosauridae (Dinosauria, Coelurosauria). *Journal of Vertebrate Paleontology* **19**: 497–520.
- Castanet J. 1987.** La squeletteochronologie chez les reptiles. III-Application. *Annales des Sciences Naturelles, Zoologie, Paris. Série 13* **8**: 157–172.
- Castanet J. 1994.** Age estimation and longevity in reptiles. *Gerontology* **40**: 174–192.
- Castanet J, Francillon-Vieillot H, Meunier FJ, de Ricqlès A. 1993.** Bone and individual aging. In: Hall BK, ed. *Bone*, Vol. 7: *bone growth B*. Boca Raton: CRC Press, 245–283.
- Chabreck RH, Joanen T. 1979.** Growth rates of American alligators in Louisiana. *Herpetologica* **35**: 51–57.
- Chinsamy A. 1990.** Physiological implications of the bone histology of *Syntarsus rhodesiensis* (Saurischia: Theropoda). *Palaeontologia Africana* **27**: 77–82.
- Chinsamy A. 1993.** Image analysis and the physiological implications of the vascularisation of femora in archosaurs. *Modern Geology* **19**: 101–108.

- Chinsamy A. 1995.** Ontogenetic changes in the bone histology of the Late Jurassic ornithomimid *Dryosaurus lettowvorbecki*. *Journal of Vertebrate Paleontology* **15**: 96–104.
- Chinsamy A, Chiappe LM, Dodson P. 1995.** Mesozoic avian bone microstructure: physiological implications. *Paleobiology* **21**: 561–574.
- Chinsamy A, Dodson P. 1995.** Inside a dinosaur bone. *American Scientist* **83**: 174–180.
- Chinsamy A, Elzanowski A. 2001.** Evolution of growth pattern in birds. *Nature* **412**: 402–403.
- Chinsamy A, Raath MA. 1992.** Preparation of fossil bone for histological examination. *Palaeontologia Africana* **29**: 39–44.
- Cohen A, Serjeantson D. 1996.** *A manual for the identification of bird bones from archaeological sites*. Revised edition. London: Archetype Publications.
- Curry KA. 1999.** Ontogenetic histology of *Apatosaurus* (Dinosauria: Sauropoda): new insights on growth rates and longevity. *Journal of Vertebrate Paleontology* **19**: 654–665.
- Dalrymple GH. 1996.** Growth of American alligators in the Shark Valley region of Everglades National Park. *Copeia* **1996**: 212–216.
- Dodson P. 1975.** Functional and ecological significance of relative growth in *Alligator*. *Journal of Zoology* **175**: 315–355.
- Elsey RM, Joanen T, McNease L, Lance V. 1990.** Growth rate and plasma corticosteroid levels in juvenile alligators maintained at different stocking densities. *Journal of Experimental Zoology* **255**: 30–36.
- Elsey RM, Lance VA, McNease L. 2000a.** Evidence of accelerated sexual maturity and nesting in farm-released alligators in Louisiana. In: Grigg GC, Seebacher F, Franklin CE, eds. *Crocodylian biology and evolution*. Chipping Norton: Surrey Beatty and Sons, 244–255.
- Elsey RM, McNease L, Joanen T. 2000b.** Louisiana's alligator ranching programme: a review and analysis of releases of captive-raised juveniles. In: Grigg GC, Seebacher F, Franklin CE, eds. *Crocodylian biology and evolution*. Chipping Norton: Surrey Beatty and Sons, 426–441.
- Enlow DH. 1969.** The bone of reptiles. In: Gans C, Bellairs A, Parsons TS, eds. *Biology of the Reptilia. Vol. 1, Morphology*. A. New York: Academic Press, 45–80.
- Enlow DH, Brown SO. 1957.** A comparative histological study of fossil and recent bone tissues. Part II. *Texas Journal of Science* **9**: 186–214.
- Farlow J, Hurlburt G, Elsey R, Britton A. 2003.** Femoral dimensions and body size of *Alligator mississippiensis*: estimating the size of fossil crocodylians and their kin. *Journal of Vertebrate Paleontology* **23**: 49A.
- Farlow JO, Hurlburt GR, Elsey RM, Britton ARC, Langston W Jr. 2005.** Femoral dimensions and body size of *Alligator mississippiensis*: estimating the size of extinct mesoeucrocodylians. *Journal of Vertebrate Paleontology* **25**: 354–369.
- Gotfredsen AB. 1997.** Sea bird exploitation on coastal Inuit sites, West and Southeast Greenland. *International Journal of Osteoarchaeology* **7**: 271–286.
- Groomsbridge B. 1987.** The distribution and status of world crocodylians. In: Webb GJW, Manolis SC, Whitehead PJ, eds. *Wildlife management: crocodiles and alligators*. Chipping Norton: Surrey Beatty and Sons, 9–21.
- Horner JR, Currie PJ. 1994.** Embryonic and neonatal morphology and ontogeny of a new species of *Hypacrosaurus* (Ornithischia: Lambeosauridae) from Montana and Alberta. In: Carpenter K, Hirsch KF, Horner JR, eds. *Dinosaur eggs and babies*. Cambridge: Cambridge University Press, 312–336.
- Horner JR, de Ricqlès A, Padian K. 2000.** Long bone histology of the hadrosaurid dinosaur *Maiasaura peeblesorum*: growth dynamics and physiology based on an ontogenetic series of skeletal elements. *Journal of Vertebrate Paleontology* **20**: 115–129.
- Horner JR, Padian K, de Ricqlès A. 2001.** Comparative osteohistology of some embryonic and perinatal archosaurs: developmental and behavioral implications for dinosaurs. *Paleobiology* **27**: 39–58.
- Huchzermeyer FW. 2002.** Stress in farmed and captive crocodiles: stressors and effects. In: *Crocodyles. Proceedings of the 16th Working Meeting of the Crocodile Specialist Group*. Gland, Switzerland and Cambridge, UK: IUCN – The World Conservation Union, 173–176.
- Hutton JM. 1986.** Age determination of living Nile crocodiles from the cortical stratification of bone. *Copeia* **1986**: 332–341.
- Jacobs LL, Winkler DA, Murry PA, Maurice JM. 1994.** A nodosaurid scuteling from the Texas shore of the Western Interior Seaway. In: Carpenter K, Hirsch KF, Horner JR, eds. *Dinosaur eggs and babies*. Cambridge: Cambridge University Press, 337–346.
- Jacobsen T, Kushlan JA. 1989.** Growth dynamics in the American alligator (*Alligator mississippiensis*). *Journal of Zoology* **219**: 309–328.
- Joanen T, McNease L. 1987a.** Alligator farming research in Louisiana, USA. In: Webb GJW, Manolis SC, Whitehead PJ, eds. *Wildlife management: crocodiles and alligators*. Chipping Norton: Surrey Beatty and Sons, 329–340.
- Joanen T, McNease L. 1987b.** The management of alligators in Louisiana, USA. In: Webb GJW, Manolis SC, Whitehead PJ, eds. *Wildlife management: crocodiles and alligators*. Chipping Norton: Surrey Beatty and Sons, 33–42.
- Johnson R. 1977.** Size independent criteria for estimating relative age and the relationships among growth parameters in a group of fossil reptiles (Reptilia: Ichthyosauria). *Canadian Journal of Earth Sciences* **14**: 1916–1924.
- Lance VA. 2003.** Alligator physiology and life history: the importance of temperature. *Experimental Gerontology* **38**: 801–805.
- Lance VA, Morici LA, Elsey RM. 2000.** Physiology and endocrinology of stress in crocodylians. In: Grigg GC, Seebacher F, Franklin CE, eds. *Crocodylian biology and evolution*. Chipping Norton: Surrey Beatty and Sons, 327–340.
- Magnusson WE, Vliet KA, Pooley AC, Whitaker R. 1989.** *Reproduction*. In: Ross CA, ed. *Crocodyles and Alligators*. New York: Facts on File, 118–135.
- Mannermaa K. 2002.** Bird bones from Jettböle I, a site in the Neolithic Åland archipelago in the northern Baltic. *Acta Zoologica Cracoviensia* **45**: 85–98.

- McIlhenny EA. 1935.** *The alligator's life history*. Boston: Christopher Publishing House.
- Meers MB. 1999.** Evolution of the crocodylian forelimb: anatomy, biomechanics, and functional morphology. PhD thesis, The Johns Hopkins University School of Medicine.
- Meers MB. 2003.** Crocodylian forelimb musculature and its relevance to Archosauria. *Anatomical Record Part A* **274A**: 891–916.
- Neill WT. 1971.** *The last of the ruling reptiles: alligators, crocodiles, and their kin*. New York: Columbia University Press.
- Padian K, Horner JR, de Ricqlès A. 2004.** Growth in small dinosaurs and pterosaurs: the evolution of archosaurian growth strategies. *Journal of Vertebrate Paleontology* **24**: 555–571.
- Peabody FE. 1961.** Annual growth zones in living and fossil vertebrates. *Journal of Morphology* **108**: 11–62.
- Reid REH. 1984.** The histology of dinosaurian bone, and its possible bearing on dinosaurian physiology. In: Ferguson MWJ, ed. *The structure, development, and evolution of reptiles*, Vol. 52. London: Academic Press, 629–663.
- Reid REH. 1990.** Zonal 'growth rings' in dinosaurs. *Modern Geology* **15**: 19–48.
- Reid REH. 1997a.** Dinosaurian physiology: the case for 'intermediate' dinosaurs. In: Farlow JO, Brett-Surman MK, eds. *The complete dinosaur*. Bloomington: Indiana University Press, 449–473.
- Reid REH. 1997b.** Histology of bones and teeth. In: Currie PJ, Padian K, eds. *Encyclopedia of dinosaurs*. New York: Academic Press, 329–339.
- Reid REH. 1997c.** How dinosaurs grew. In: Farlow JO, Brett-Surman MK, eds. *The complete dinosaur*. Bloomington: Indiana University Press, 403–413.
- Richardson KC, Webb G, Manolis SC. 2002.** *Crocodiles inside out: a guide to the crocodilians and their functional morphology*. Chipping Norton: Surrey Beatty and Sons.
- de Ricqlès AJ. 1974.** Evolution of endothermy: histological evidence. *Evolutionary Theory* **1**: 51–80.
- de Ricqlès AJ. 1976.** On bone histology of fossil and living reptiles, with comments on its functional and evolutionary significance. In: Bellairs A, Cox CB, eds. *Morphology and biology of reptiles*. New York: Academic Press, 123–151.
- de Ricqlès AJ, Padian K, Horner JR. 1993.** Paleohistology of pterosaur bones. *Journal of Vertebrate Paleontology* **13**: 54A.
- de Ricqlès A, Padian K, Horner JR. 2001.** The bone histology of basal birds in phylogenetic and ontogenetic perspectives. In: Gauthier J, Gall LF, eds. *New perspectives on the origin and early evolution of birds: Proceedings of the International Symposium in Honor of John H. Ostrom*. New Haven: Peabody Museum of Natural History, Yale University, 411–426.
- de Ricqlès AJ, Padian K, Horner JR, Francillon-Vieillot H. 2000.** Palaeohistology of the bones of pterosaurs (Reptilia: Archosauria): anatomy, ontogeny and biomechanical implications. *Zoological Journal of the Linnean Society* **129**: 349–385.
- de Ricqlès AJ, Padian K, Horner JR, Lamm E-T, Myhrvold N. 2003.** Osteohistology of *Confuciusornis sanctus* (Theropoda: Aves). *Journal of Vertebrate Paleontology* **23**: 373–386.
- Romer AS. 1923.** Crocodilian pelvic muscles and their avian and reptilian homologues. *American Museum of Natural History Bulletin* **48**: 533–552, Plates XIX–XXV.
- Rootes WL, Chabreck RH, Wright VL, Brown BW, Hess TJ. 1991.** Growth rates of American alligators in estuarine and palustrine wetlands in Louisiana. *Estuaries* **14**: 489–494.
- Ross JP, Hinterkopf JP, Honeyfield DC, Carbonneau D, Woodward A, Sepulveda M, Gross T. 2002.** Thiamine status and mortality of adult American alligators (*Alligator mississippiensis*) in Lakes Griffin and Woodruff in central Florida during 2000 and 2001. In: *Crocodiles. Proceedings of the 16th Working Meeting of the Crocodile Specialist Group*. Gland, Switzerland and Cambridge, UK: IUCN – the World Conservation Union, 189–190.
- Ryan MJ, Russell AP. 2005.** A new centrosaurine ceratopsid from the Oldman Formation of Alberta and its implications for centrosaurine taxonomy and systematics. *Canadian Journal of Earth Sciences* **42**: 1369–1387.
- Ryan MJ, Russell AP, Eberth DA, Currie PJ. 2001.** The taphonomy of a *Centrosaurus* (Ornithischia: Ceratopsidae) bone bed from the Dinosaur Park Formation (Upper Campanian), Alberta, Canada, with comments on cranial ontogeny. *Palaios* **16**: 482–506.
- Sack WO, Habel RE, eds. 1994.** *Nomina Anatomica Veterinaria/Nomina Histologica/Nomina Embryologica Veterinaria*. World Association of Veterinary Anatomists.
- Sampson SD, Ryan MJ, Tanke DH. 1997.** Craniofacial ontogeny in centrosaurine dinosaurs (Ornithischia: Ceratopsidae): taxonomic and behavioral implications. *Zoological Journal of the Linnean Society* **121**: 293–337.
- Sander PM. 2000.** Longbone histology of the Tendaguru sauropods: implications for growth and biology. *Paleobiology* **26**: 466–488.
- Sanz JL, Chiappe LM, Pérez-Moreno BP, Moratalla JJ, Hernández-Carrasquilla F, Buscalioni AD, Ortega F, Poyato-Ariza FJ, Rasskin-Gutman D, Martínez-Delclòs X. 1997.** A nestling bird from the Lower Cretaceous of Spain: implications for avian skull and neck evolution. *Science* **276**: 1543–1546.
- Schoeb TR, Heaton-Jones TG, Clemmons RM, Carbonneau DA, Woodward AR, Shelton D, Poppenga RH. 2002.** Clinical and necropsy findings associated with increased mortality among American alligators of Lake Griffin, Florida. *Journal of Wildlife Diseases* **38**: 320–337.
- Serjeantson D. 1998.** Birds: a seasonal resource. *Environmental Archaeology* **3**: 23–33.
- Serjeantson D. 2002.** Goose husbandry in Medieval England, and the problem of ageing goose bones. *Acta Zoologica Cracoviensia* **45**: 39–54.
- Swofford DL. 1999.** *PAUP* Phylogenetic Analysis Using Parsimony*, Version 4. Sunderland, MA: Sinauer Associates.
- Tucker AD. 1997.** Validation of skeletochronology to determine age of freshwater crocodiles (*Crocodylus johnstoni*). *Marine and Freshwater Research* **48**: 343–351.

- Tumarkin-Deratzian AR, Vann DR, Dodson P. 2006.** Bone surface texture as an ontogenetic indicator in long bones of the Canada goose *Branta canadensis* (Anseriformes: Anatidae). *Zoological Journal of the Linnean Society* **148**: 133–168.
- Varricchio DJ. 1993.** Bone microstructure of the Upper Cretaceous theropod dinosaur *Troodon formosus*. *Journal of Vertebrate Paleontology* **13**: 99–104.
- Wilkinson PM, Rhodes WE. 1997.** Growth rates of American alligators in coastal South Carolina. *Journal of Wildlife Management* **61**: 397–402.
- Wink CS, Elsey RM. 1986.** Changes in femoral morphology during egg-laying in *Alligator mississippiensis*. *Journal of Morphology* **189**: 183–188.
- Wink CS, Elsey RM, Hill EM. 1987.** Changes in femoral robusticity and porosity during the reproductive cycle of the female alligator (*Alligator mississippiensis*). *Journal of Morphology* **193**: 317–321.
- Woodward AR, White JH, Linda SB. 1995.** Maximum size of the alligator (*Alligator mississippiensis*). *Journal of Herpetology* **29**: 507–513.

APPENDIX 1

Character list for size-independent maturity estimates, modified after Brochu (1992, 1996). All characters scored as 0 = absent, 1 = present

Femur

- 1 Medial scar for M. puboischiofemoralis internus, pars dorsalis
- 2 Lateral scar for M. puboischiofemoralis internus, pars dorsalis
- 3 Proximal dorsal tuberosity
- 4 Distal trochlea
- 5 Medial and lateral sides of distal condyle rugose
- 6 Primary adductor scar
- 7 Longitudinal scars for M. iliofemoralis
- 8 Secondary adductor scar
- 9 Tertiary longitudinal scar
- 10 Distinct scar for M. puboischiofemoralis internus, pars medialis

Tibia

- 1 Scar for M. flexor tibialis interior
- 2 Scar for medial tibioastragalar ligament
- 3 Scar for M. interosseus cruris
- 4 Scar for internal lateral ligament
- 5 Ridge for M. tibialis cranialis extending from M. flexor tibialis interior scar
- 6 Assemblage of scars for M. tibialis caudalis, M. tibialis cranialis, and femorotibial ligament
- 7 Scars for femorotibial ligament and M. tibialis caudalis distinct from above assemblage
- 8 Scar for M. tibialis cranialis distinct from above assemblage
- 9 Posterior ridge for M. flexor digitorum longus

Humerus

- 1 Scar for M. teres major and branch of M. latissimus dorsi
- 2 Scar for M. anconaeus humeralis caudalis
- 3 Scar for M. humeroradialis
- 4 Scar for M. anconaeus humeralis medialis
- 5 Scar for M. humeroantibrachialis inferior
- 6 Distal trochlea
- 7 Rugose tip to deltopectoral crest
- 8 Scar for M. scapulohumeralis profundus
- 9 Scar for M. coracobrachialis

APPENDIX 2

Composition of cluster analysis Groups listed on Figure 3

Femur

Group 1

ROM R6251
ROM R6252
ROM R6253

Group 2

MOR HIP2001-08R-52
MOR HIP2001-08R-57
MOR HIP2001-08R-60
MOR HIP2001-08R-63
MOR HIP2001-08R-64
MOR HIP2001-08R-65
MOR HIP2001-08R-66
MOR HIP2001-08R-67
MOR HIP2001-08R-69
UF 35144
UF 35145
UF 35146
UF 35148
UF 35149
UF 35151
UF 38973
UF 42475
UF 42538

Group 3

FWC 35119
FWC 40723
FWC 40859
FWC LGS7
MOR HIP2001-08R-2
MOR HIP2001-08R-3
MOR HIP2001-08R-6
MOR HIP2001-08R-8
MOR HIP2001-08R-10
MOR HIP2001-08R-11
MOR HIP2001-08R-13
MOR HIP2001-08R-16
MOR HIP2001-08R-17
MOR HIP2001-08R-18
MOR HIP2001-08R-19
MOR HIP2001-08R-20
MOR HIP2001-08R-23
MOR HIP2001-08R-25
MOR HIP2001-08R-26
MOR HIP2001-08R-27
MOR HIP2001-08R-28
MOR HIP2001-08R-29
MOR HIP2001-08R-30
MOR HIP2001-08R-32
MOR HIP2001-08R-35
MOR HIP2001-08R-36
MOR HIP2001-08R-37
MOR HIP2001-08R-38
MOR HIP2001-08R-39
MOR HIP2001-08R-40
MOR HIP2001-08R-41
MOR HIP2001-08R-44
MOR HIP2001-08R-45
MOR HIP2001-08R-49
MOR HIP2001-08R-50
MOR HIP2001-08R-51
MOR HIP2001-08R-53
MOR HIP2001-08R-55
MOR HIP2001-08R-56
MOR HIP2001-08R-59
MOR HIP2001-08R-61
MOR HIP2001-08R-62
MOR HIP2001-08R-68
ROM R4409
ROM R4413
ROM R4415
ROM R4416
UF 35155
UF 37230
UF 109039

Group 4

MOR HIP2001-08R-1
MOR HIP2001-08R-4
MOR HIP2001-08R-5
MOR HIP2001-08R-7
MOR HIP2001-08R-9
MOR HIP2001-08R-15
MOR HIP2001-08R-22
MOR HIP2001-08R-42
MOR HIP2001-08R-43
MOR HIP2001-08R-47

APPENDIX 2 *Continued*

Tibia		
<i>Group 1</i>	<i>Group 2</i>	<i>Group 3</i>
ROM R6251	UF 35144	FWC 35119
	UF 35145	FWC 40723
	UF 35146	FWC 40859
	UF 35148	FWC LGS7
	UF 35149	ROM R4409
	UF 35151	ROM R4413
	UF 38973	ROM R4415
	UF 42475	ROM R4416
	UF 42538	UF 35155
		UF 37230
		UF 109039
Humerus		
<i>Group 1</i>	<i>Group 2</i>	<i>Group 3</i>
ROM R6251	UF 35144	FWC 35119
ROM R6252	UF 35145	FWC 40723
ROM R6253	UF 35146	FWC 40859
	UF 35148	FWC LGS7
	UF 35151	ROM R4409
		ROM R4413
		ROM R4415
		ROM R4416
		UF 35149
		UF 35155
		UF 37230
		UF 38973
		UF 42538
		UF 109039

APPENDIX 3

Bone landmark character matrices for size-independent analyses. Character numbers and codes correspond to descriptions in Appendix 1. '?' indicates missing data. Only those specimens marked with an * were used in the parsimony analyses. ROM R4406 was known from the humerus only; it was not included in the cluster analyses or textural investigations

Specimen number		Character no.								
		1	2	3	4	5	6	7	8	9
<i>Femur</i>										
*Outgroup		0	0	0	0	0	0	0	0	0
*FWC	35119	1	1	1	1	1	1	1	1	0
*FWC	40583	1	1	1	1	1	1	1	1	0
FWC	40723	1	1	1	1	1	1	1	1	0
FWC	40853	1	1	1	1	1	1	1	1	0
*FWC	40854	1	1	1	1	1	1	1	1	1
FWC	40859	1	1	1	1	1	1	1	1	0
FWC	LGS1	1	1	1	1	1	1	1	1	1
FWC	LGS2	1	1	1	1	1	1	1	1	1

APPENDIX 3 *Continued*

		Character no.									1
Specimen number		1	2	3	4	5	6	7	8	9	0
FWC	LGS3	1	1	1	1	1	1	1	1	1	1
FWC	LGS4	1	1	1	1	1	1	1	1	1	1
FWC	LGS5	1	1	1	1	1	1	1	1	1	1
FWC	LGS6	1	1	1	1	1	1	1	1	1	1
FWC	LGS7	1	1	1	1	1	1	1	1	1	0
FWC	LGS8	1	1	1	1	1	1	1	1	1	1
MOR	HIP2001-08R-1	1	1	1	1	1	1	1	1	1	1
MOR	HIP2001-08R-2	1	1	1	1	1	1	1	1	1	0
MOR	HIP2001-08R-3	1	1	1	1	1	1	1	1	1	0
MOR	HIP2001-08R-4	1	1	1	1	1	1	1	1	1	1
MOR	HIP2001-08R-5	1	1	1	1	1	1	1	1	1	1
MOR	HIP2001-08R-6	1	1	1	1	1	1	1	1	1	0
MOR	HIP2001-08R-7	1	1	1	1	1	1	1	1	1	1
MOR	HIP2001-08R-8	1	1	1	1	1	1	1	1	1	0
MOR	HIP2001-08R-9	1	1	1	1	1	1	1	1	1	1
MOR	HIP2001-08R-10	1	1	1	1	1	1	1	1	1	0
MOR	HIP2001-08R-11	1	1	1	1	1	1	1	1	1	0
MOR	HIP2001-08R-13	1	1	1	1	1	1	1	1	1	0
MOR	HIP2001-08R-15	1	1	1	1	1	1	1	1	1	1
MOR	HIP2001-08R-16	1	1	1	1	1	1	1	1	1	0
MOR	HIP2001-08R-17	1	1	1	1	1	1	1	1	1	0
MOR	HIP2001-08R-18	1	1	1	1	1	1	1	1	1	0
MOR	HIP2001-08R-19	1	1	1	1	1	1	1	1	1	0
MOR	HIP2001-08R-20	1	1	1	1	1	1	1	1	1	0
MOR	HIP2001-08R-22	1	1	1	1	1	1	1	1	1	1
MOR	HIP2001-08R-23	1	1	1	1	1	1	1	1	1	0
MOR	HIP2001-08R-25	1	1	1	1	1	1	1	1	1	0
MOR	HIP2001-08R-26	1	1	1	1	1	1	1	1	1	0
MOR	HIP2001-08R-27	1	1	1	1	1	1	1	1	1	0
MOR	HIP2001-08R-28	1	1	1	1	1	1	1	1	1	0
MOR	HIP2001-08R-29	1	1	1	1	1	1	1	1	1	0
MOR	HIP2001-08R-30	1	1	1	1	1	1	1	1	1	0
MOR	HIP2001-08R-32	1	1	1	1	1	1	1	1	1	0
MOR	HIP2001-08R-35	1	1	1	1	1	1	1	1	1	0
MOR	HIP2001-08R-36	1	1	1	1	1	1	1	1	1	0
MOR	HIP2001-08R-37	1	1	1	1	1	1	1	1	1	0
MOR	HIP2001-08R-38	1	1	1	1	1	1	1	1	1	0
MOR	HIP2001-08R-39	1	1	1	1	1	1	1	1	1	0
MOR	HIP2001-08R-40	1	1	1	1	1	1	1	1	1	0
MOR	HIP2001-08R-41	1	1	1	1	1	1	1	1	1	0
MOR	HIP2001-08R-42	1	1	1	1	1	1	1	1	1	1
MOR	HIP2001-08R-43	1	1	1	1	1	1	1	1	1	1
MOR	HIP2001-08R-44	1	1	1	1	1	1	1	1	1	0
MOR	HIP2001-08R-45	1	1	1	1	1	1	1	1	1	0
MOR	HIP2001-08R-47	1	1	1	1	1	1	1	1	1	1
MOR	HIP2001-08R-49	1	1	1	1	1	1	1	1	1	0
MOR	HIP2001-08R-50	1	1	1	1	1	1	1	1	1	0
MOR	HIP2001-08R-51	1	1	1	1	1	1	1	1	1	0
*MOR	HIP2001-08R-52	1	1	1	1	1	1	1	1	0	0
MOR	HIP2001-08R-53	1	1	1	1	1	1	1	1	1	0
MOR	HIP2001-08R-55	1	1	1	1	1	1	1	1	1	0

APPENDIX 3 *Continued*

Specimen number		Character no.									1
		1	2	3	4	5	6	7	8	9	0
MOR	HIP2001-08R-56	1	1	1	1	1	1	1	1	1	0
MOR	HIP2001-08R-57	1	1	1	1	1	1	1	1	0	0
MOR	HIP2001-08R-59	1	1	1	1	1	1	1	1	1	0
*MOR	HIP2001-08R-60	1	1	1	1	1	0	1	1	0	0
MOR	HIP2001-08R-61	1	1	1	1	1	1	1	1	1	0
MOR	HIP2001-08R-62	1	1	1	1	1	1	1	1	1	0
MOR	HIP2001-08R-63	1	1	1	1	1	1	1	1	0	0
*MOR	HIP2001-08R-64	1	1	1	1	1	1	1	0	0	0
*MOR	HIP2001-08R-65	1	1	0	1	1	1	1	1	0	0
MOR	HIP2001-08R-66	1	1	1	1	1	1	1	1	0	0
MOR	HIP2001-08R-67	1	1	1	1	1	1	1	0	0	0
MOR	HIP2001-08R-68	1	1	1	1	1	1	1	1	1	0
MOR	HIP2001-08R-69	1	1	1	1	1	1	1	0	0	0
ROM	R4401	1	1	1	1	1	1	1	1	1	0
ROM	R4402	1	1	1	1	1	1	1	1	1	1
ROM	R4404	1	1	1	1	1	1	1	1	1	0
ROM	R4405	1	1	1	1	1	1	1	1	1	0
ROM	R4407	1	1	1	1	1	1	1	1	1	0
ROM	R4408	1	1	1	1	1	1	1	1	1	1
ROM	R4409	1	1	1	1	1	1	1	1	1	0
ROM	R4413	1	1	1	1	1	1	1	1	1	0
ROM	R4415	1	1	1	1	1	1	1	1	1	0
ROM	R4416	1	1	1	1	1	1	1	1	1	0
*ROM	R6251	1	0	0	0	0	0	0	0	0	0
*ROM	R6252	1	1	0	0	0	1	0	1	0	0
ROM	R6253	1	0	0	0	0	0	0	0	0	0
UF	33552	1	1	1	1	1	1	1	1	1	1
UF	35144	1	1	0	1	1	1	1	0	0	0
*UF	35145	1	1	0	1	1	1	1	0	0	0
*UF	35146	1	1	0	1	1	1	1	0	1	0
UF	35147	1	1	0	1	1	1	1	0	0	0
UF	35148	1	1	0	1	1	1	1	0	0	0
UF	35149	1	1	0	1	1	1	1	1	0	0
*UF	35150	1	1	0	1	1	1	1	1	1	0
UF	35151	1	1	0	1	1	1	1	0	0	0
UF	35155	1	1	1	1	1	1	1	1	1	0
UF	37230	1	1	1	1	1	1	1	1	1	0
UF	37231	1	1	1	1	1	1	1	1	1	1
UF	38973	1	1	0	1	1	1	1	1	0	0
UF	38974	1	1	1	1	1	1	1	1	1	0
UF	40535	1	1	0	1	1	1	1	1	0	0
UF	42474	1	1	0	1	1	1	1	1	1	0
UF	42475	1	1	0	1	1	1	1	1	0	0
*UF	42523	1	1	0	1	1	1	1	1	0	1
UF	42538	1	1	0	1	1	1	1	1	0	0
UF	67824	1	1	1	1	1	1	1	1	1	0
UF	87885	1	1	1	1	1	1	1	1	1	0
UF	98341	1	1	1	1	1	1	1	1	1	0
UF	109039	1	1	0	1	1	1	1	1	1	0
*UF	109040	1	1	1	1	1	1	1	0	1	0

APPENDIX 3 *Continued*

		Character no.									1 0
		1	2	3	4	5	6	7	8	9	
Specimen number		1	2	3	4	5	6	7	8	9	
<i>Tibia</i>											
*Outgroup		0	0	0	0	0	0	0	0	0	
FWC	35119	1	1	1	1	1	1	0	0	1	
FWC	40583	1	1	1	1	1	1	0	0	1	
FWC	40723	1	1	1	1	1	1	0	0	1	
FWC	40853	1	1	1	1	1	1	0	1	1	
FWC	40854	1	1	1	1	1	1	0	0	1	
*FWC	40859	1	1	1	1	1	1	?	?	1	
FWC	LGS2	1	1	1	1	1	1	0	0	1	
*FWC	LGS3	1	1	1	1	1	1	0	0	1	
FWC	LGS4	1	1	1	1	1	1	0	1	1	
FWC	LGS7	1	1	1	1	1	1	0	0	1	
FWC	LGS8	1	1	1	1	1	1	0	0	1	
ROM	R4401	1	1	1	1	1	1	1	1	1	
ROM	R4402	1	1	1	1	1	1	0	0	1	
ROM	R4405	1	1	1	1	0	1	0	1	1	
ROM	R4407	1	1	1	1	0	1	0	0	1	
*ROM	R4408	1	1	1	1	0	1	0	1	1	
ROM	R4409	1	1	1	1	1	1	0	0	1	
ROM	R4413	1	1	1	1	1	1	0	0	1	
ROM	R4415	1	1	1	1	1	1	0	0	1	
ROM	R4416	1	1	1	1	1	1	0	0	1	
*ROM	R6251	0	0	0	0	0	0	0	0	1	
UF	33552	1	1	1	1	1	1	1	1	1	
UF	35144	1	1	1	1	0	1	0	0	1	
UF	35145	1	1	1	1	0	1	0	0	1	
UF	35146	1	1	1	1	0	1	0	0	0	
UF	35147	1	1	1	1	1	1	0	0	1	
UF	35148	1	1	1	1	0	1	0	0	1	
*UF	35149	1	1	1	1	0	1	0	0	1	
*UF	35150	1	1	1	1	0	1	0	0	0	
UF	35151	1	1	1	1	0	1	0	0	1	
UF	35155	1	1	1	1	1	1	0	0	1	
*UF	37230	1	1	1	1	1	1	0	1	1	
UF	37231	1	1	1	1	1	1	0	0	1	
UF	38973	1	1	1	1	0	1	0	0	1	
UF	38974	1	1	1	1	1	1	0	0	1	
*UF	40535	1	1	1	1	0	1	1	1	1	
UF	42474	1	1	1	1	0	1	0	0	1	
UF	42475	1	1	1	1	0	1	0	0	1	
*UF	42523	0	1	1	1	0	1	0	0	1	
*UF	42538	1	1	1	1	0	1	1	0	1	
UF	67824	1	1	1	1	1	1	0	1	1	
*UF	87885	1	1	1	1	1	1	1	1	1	
UF	98341	1	1	1	1	1	1	1	1	1	
UF	109039	1	1	1	1	1	1	0	0	1	
UF	109040	1	1	1	1	1	1	0	0	1	

APPENDIX 3 *Continued*

Specimen number		Character no.								
		1	2	3	4	5	6	7	8	9
<i>Humerus</i>										
*Outgroup		0	0	0	0	0	0	0	0	0
*FWC	35119	1	1	1	1	0	1	1	0	0
FWC	40583	1	1	1	1	0	1	1	0	0
FWC	40723	1	1	1	1	0	1	1	0	0
FWC	40853	1	1	1	1	0	1	1	0	1
FWC	40854	1	1	1	1	1	1	1	1	1
FWC	40859	1	1	1	1	0	1	1	0	0
FWC	LGS2	1	1	1	1	0	1	1	0	1
FWC	LGS3	1	1	1	1	0	1	1	0	0
*FWC	LGS4	1	1	1	1	0	1	1	0	1
FWC	LGS7	1	1	1	1	0	1	1	0	0
*FWC	LGS8	1	1	1	1	1	1	1	1	1
ROM	R4401	1	1	1	1	0	1	1	0	0
*ROM	R4402	1	1	1	1	1	1	1	1	0
ROM	R4404	1	1	1	1	0	1	1	0	0
ROM	R4405	1	1	1	1	0	1	1	0	0
*ROM	R4406	1	1	1	1	1	1	1	0	0
ROM	R4407	1	1	1	1	0	1	1	0	0
ROM	R4408	1	1	1	1	1	1	1	0	0
ROM	R4409	1	1	1	1	0	1	1	0	0
ROM	R4413	1	1	1	1	0	1	1	0	0
ROM	R4415	1	1	1	1	0	1	1	0	0
ROM	R4416	1	1	1	1	1	1	1	0	0
*ROM	R6251	0	1	0	0	0	0	0	0	0
ROM	R6252	0	0	0	0	0	0	0	0	0
*ROM	R6253	0	1	0	0	0	1	1	0	0
UF	33552	1	1	1	1	1	1	1	1	1
*UF	35144	1	0	1	0	0	1	0	0	0
*UF	35145	1	0	1	0	0	1	1	0	0
UF	35146	1	1	1	0	0	1	1	0	0
UF	35147	1	1	1	0	0	1	1	0	0
*UF	35148	1	1	1	0	0	1	1	0	0
UF	35149	1	0	1	1	0	1	1	0	0
UF	35150	1	0	1	1	0	1	1	0	0
UF	35151	1	0	1	0	0	1	1	0	0
*UF	35155	1	1	1	1	0	0	1	0	0
UF	37230	1	1	1	1	0	1	1	0	0
UF	37231	1	1	1	1	0	1	1	0	0
UF	38973	1	1	1	1	0	1	1	0	0
UF	38974	1	1	1	1	0	1	1	0	0
UF	40535	1	1	1	1	0	1	1	0	0
UF	42474	1	0	1	0	0	1	1	0	0
*UF	42475	1	1	1	1	0	1	1	1	0
UF	42523	1	0	1	1	0	1	1	0	0
*UF	42538	1	0	1	1	0	1	1	0	0
UF	67824	1	1	1	1	0	1	1	0	1
UF	87885	1	1	1	1	0	1	1	1	0
UF	98341	1	1	1	1	1	1	1	0	0
UF	109039	1	1	1	1	0	1	1	0	0
UF	109040	1	1	1	1	0	1	1	0	0